Modelling the formation of linear geochemical trends using the Magma Chamber Simulator: a case study of the Jindabyne granitoids, Lachlan Fold Belt, Australia

Iles, Kieran A.

2022-01

Iles , K A & Heinonen , J S 2022 , ' Modelling the formation of linear geochemical trends using the Magma Chamber Simulator: a case study of the Jindabyne granitoids, Lachlan Fold Belt, Australia ' , Journal of Petrology , vol. 63 , no. 1 , egab102 . https://doi.org/10.1093/petrology/egab102

http://hdl.handle.net/10138/340791
https://doi.org/10.1093/petrology/egab102

JOURNAL OF PETROLOGY

Journal of Petrology, 2022, Vol. 63, No. 1, 1–33
https://doi.org/10.1093/petrology/egab102
Advance Access Publication Date: 10 December 2021
Original Manuscript

OXFORD

Modelling the Formation of Linear Geochemical Trends Using the Magma Chamber Simulator: A Case Study of the Jindabyne Granitoids, Lachlan Fold Belt, Australia

Kieran A. Iles* and Jussi S. Heinonen

Department of Geosciences and Geography, University of Helsinki, P.O. Box 64, 00014 Helsinki, Finland

*Corresponding author: Telephone: +358451598844, E-mail: kieran.iles@helsinki.fi

Received 9 August 2019; Revised 3 December 2021; Accepted 4 December 2021

Abstract

Understanding the origins of major and trace element variations and the isotopic character of granite samples in terms of sources and magmatic processes is, arguably, the core of granite petrology. It is central to attempts to place these rocks in the context of broader geologic processes and continent evolution. For the granites of the Lachlan and New England Fold Belts (LFB and NEFB) of Australia there has been great debate between competing petrogenetic models. The open-system view is that the isotopic variability and within-suite compositional trends can be accounted for by magma mixing, assimilation and fractional crystallisation (FC). In contrast, the restite unmixing model views the isotope compositions of diverse granites as a feature inherited from individual protoliths that underwent partial melting to produce magmas entraining varying proportions of residual material in a felsic melt. Reconciling all aspects of the geochemical data in a mixing model is contingent on a plausible fractionation regime to produce the observed consistently linear (or near-linear) trends on Harker diagrams; however, published FC models lack phase equilibria constraints on the liquidus assemblage and do not account for the likely changes in trace element partitioning across the modelled compositional range. The Magma Chamber Simulator (MCS) can be used to model fractional crystallisation alone (FC) or with assimilation (AFC), constraining phase equilibria and accounting for the thermal budget. Here, this tool was used to conduct a case study of the I-type Jindabyne Suite of granites from the LFB, testing whether thermodynamically feasible geochemical trends matching the observed linear variations can arise through FC (with or without assimilation of supracrustal material). The results of 112 MCS models show: (1) that major element liquid lines of descent (LLDs) may be sensibly linear over limited compositional ranges, (2) that the involvement of assimilation extends the range in which trends are relatively simple and near-linear, and (3) that, despite these observations, neither FC nor AFC are able to correctly reproduce the geochemical evolution of the I-type Jindabyne Suite granitoids as an LLD (contrary to existing models)—instead, these processes persistently produce curved and kinked trends. The output of these simulations were further refined to explore models in which: (1) crystal-bearing magmas evolve via FC or AFC (with chemical isolation assumed to be achieved through crystal zoning) and undergo varying degrees of melt-crystal segregation at different stages to produce the sample compositions, and (2) *in situ* crystallisation occurs via FC within the crystallisation zone, driving the evolution of a liquid resident magma, which the samples represent. These models *are* able to reproduce the Jindabyne Suite trends reasonably well. The modelling implies that FC, or some variant thereof, is a viable explanation for the linear trends in Jindabyne; however, tendency for grossly non-linear LLDs highlights that it should not

be assumed that FC can generally explain linear trends in granites without careful modelling such as shown here.

Key words: assimilation; fractional crystallisation; geochemical modelling; granite; magma chamber simulator

INTRODUCTION

The broad scientific question 'how do granites form?' is intrinsically linked to questions such as 'what do granites tell us about the structure and physical state of the continental crust?' and 'how has the Earth's crust grown and evolved through time?' Central to such questions is understanding the causes of geochemical diversity in granites. This is a complex problem that encompasses a wide assortment of patterns of geochemical variation (clusters vs. trends, linear vs. kinked vs. curved trends, tight vs. diffuse data) at diverse sampling scales from individual crystals to magmatic provinces, integrated with consideration of numerous geological processes that are potentially at play (melting, magma mixing, restite unmixing, fractional crystallisation, assimilation and other crystallisation-differentiation processes).

The cause of linear trends on bivariate major and trace element plots within individual granitoid plutons (or suites of related plutons) has been the subject of many studies and the source of long and ongoing debate (Chappell *et al.*, 1987; Wall *et al.*, 1987; Nishimura & Yanagi, 2000; Clemens & Stevens, 2012; Dorais & Spencer, 2014; Hertogen & Mareels, 2016; Zhao *et al.*, 2018). Two closely related models to account for granitoids with such trends are fractional crystallisation (FC) and assimilation coupled with fractional crystallisation (AFC). Whether linear trends can in general be produced in this way is a question of potentially wide interest to igneous petrologists. While it is likely not possible to comprehensively answer such a broad question in a single study, examining this issue with respect to a case study has the potential to provide insight into the generation of geochemical variation for many granitoid systems. The Jindabyne Suite of the Lachlan Fold Belt (LFB), Australia, has been chosen as the focus of this study. Such an investigation requires consideration of a set of subproblems that could benefit from a modern petrological approach that incorporates thermal and phase equilibria constraints.

Research concerning the granites (sensu lato, used throughout, encompassing plutonic rocks with the same quartz content as granites sensu stricto in the Quartz-Alkali feldspar-Plagioclase ternary diagram of Le Maitre, 2002) of the LFB and New England Fold Belts (NEFB) of Australia has centred on the cause of the geochemical variations between and within granite plutons and suites. Recognising that partial melting of quartz-feldspar-H_2O-bearing rocks will result in granitic melt and an assemblage of residual phases, White & Chappell (1977) proposed the 'restite' model to explain systematic variations observed in granitic plutons in the LFB and NEFB, and, particularly, why the granite suites are so dominantly characterised by consistent linear geochemical trends among major and trace elements on bivariate element plots. A similar idea has also been suggested by Collins *et al.* (2020) as a mechanism relevant to the Cordilleran batholiths. Diametrically opposed to the restite model interpretation of the LFB granites are various open system models for granite formation. As will be seen, the issue of differentiation mechanisms to explain the linear trends is closely linked with the debate between open vs. closed system petrogenetic models for the LFB granites.

The following sections: (1) describe the restite unmixing model and its plausibility as an alternative to FC/AFC as the cause of the observed within-suite trends in the LFB granites, (2) overview key open-system models that invoke FC/AFC, and (3) establish a conceptual framework for how FC/AFC would generate the observed within-suite trends, including the perspective of existing models. The way the Magma Chamber Simulator (MCS; Bohrson *et al.*, 2014; Bohrson *et al.*, 2020) can be used to model FC/AFC processes will be overviewed in the Methods section.

Restite unmixing

The restite model (Table 1) proposes that melting of a crustal source results in a crystal-rich magma that undergoes liquid-crystal separation, or 'unmixes', producing compositions defined by varying proportions of melt and the restitic mineral assemblage (Chappell *et al.*, 1987; Chappell & Stephens, 1988; White & Chappell, 1988). Compositions produced by the strict operation of this 'unmixing' would be linearly related; therefore, regressions of the observed linear trends on bivariate element plots should extend to the composition of the melt, in one direction, and through the bulk composition of the source rock to the bulk restite composition, in the other direction, as shown in Fig. 1a.

Whether isotope data are consistent with the restite model has been debated extensively, much of which is reviewed by Iles *et al.* (2020). Since the restite model proposes that granite suites are each derived from a particular source rock, the bulk-rock isotope compositions of a suite are expected to cluster about a single composition (Fig. 2a). While some suites show relatively large within-suite bulk-rock isotopic variability, in the restite model the isotopic variability of the source is also expected to be reflected in the variability of bulk-rock samples. The curved array in Sr-Nd isotope space suggests the variability between the granite suites reflects mixing of two or more isotopically distinct magmas from different sources (e.g. mantle and continental crust); however, this is an *inter*-suite feature that could reflect the diversity of crustal source regions, not an *intra*-suite feature, such as the linear trends which are the subject of this study. These and more isotope data are detailed in the Supplementary Material and overviewed in later sections. In addition, various studies of isotopic disequilibrium during partial melting (Hogan & Sinha, 1991; Zeng *et al.*, 2005; Farina & Stevens, 2011; Tang *et al.*, 2014; Iles *et al.*, 2018) suggest that isotopic diversity should be expected in granites derived from crustal sources and does not necessarily require open-system models. Thus, the restite model is regarded as a viable explanation for geochemical variations in granite suites. Whether it alone should be the favoured model for a particular suite or group of suites depends upon whether or not an alternative differentiation mechanism, such as AFC, is: (1) compatible with the major and trace element trends, and (2) compatible with some model for all of the observations.

Open-system models in the lachlan fold belt

Magma mixing models can readily explain isotopic variations between suites, within suites and within samples by invoking hybridisation processes in magma genesis (c.f. the restite model, above), but frequently rely on FC to account for petrographic

Table 1: Summary of models for LFB granite production and magma differentiation

Model	Origin of parental magma	Cause of linear trends	Physical state of granite magma	Cause of isotopic heterogeneity *within* suites	Cause of isotopic heterogeneity *between* suites	Model details
Restite unmixing	Partial melting of crustal source rock	Restite unmixing	Crystal-liquid mixtures	Variability in the source propagated into magma variability.	Differences in the isotopic composition of source.	Granites occur on liquid-crystal segregation (melt-restite unmixing) lines. Granite magmas should all be no more mafic than source rock, since such compositions would represent melt-depleted residua.
Wall *et al.* (1987) general FC argument	Unspecified	Fractional crystallisation[1]	Liquid[1]	Unspecified. Only variability initially present in melt can be explained.	Unspecified	All elements generalised to a small set of variations in D values. All granites generalised to 4 combinations of peraluminosity and parental SiO_2
Wall *et al.* (1987) Jindabyne models	Unspecified	Fractional crystallisation	Liquid; samples with $SiO_2 < 55.5$ wt% are cumulate	Unspecified. Only variability initially present in melt can be explained.	Unspecified	Major elements modelled by best-fit mass balance, removing plag-cpx-opx-mgt. Rb, Sr, Ba and Ni modelled by Rayleigh fractionation with phase proportion constraints form major element model.
Three component mixing	Mixing of mantle-derived mafic magma, magma derived from lower-crustal igneous lithologies and partially molten sedimentary rocks	Fractional crystallisation	Liquid in Collins (1996), but crystal-liquid mixtures in Collins (1998)[2]	Inherent to parental magma being a mixture, potentially not perfectly homogenised.	Differences in proportions of the three mixing endmembers; also possible variations in the isotopic composition of the crustal components.	Collins (1996) refers to major and trace element models such as Wall *et al.* (1987) and used similar approach to model the Moruya Suite. The parental magma for fractionation is the mafic end of a granite suite. Collins (1996) models S-type parental magma major and trace element compositions as mixtures between ≈70% Cooma diatexite and I-type tonalite represented by the Jindabyne parental magma. Keay *et al.* (1997) models the Sr-Nd isotope variation of the LFB granites as mixing lines joining three endmembers.

(Continued)

Table 1: Continued

Model	Origin of parental magma	Cause of linear trends	Physical state of granite magma	Cause of isotopic heterogeneity *within* suites	Cause of isotopic heterogeneity *between* suites	Model details
Kemp *et al.* (2005) Jindabyne model	Partial melting of igneous crustal source	Varying degrees of partial melting of source and assimilation of sediment or S-type granite	Mostly liquid with minor restitic, xenocrystic and phenocrystic material	Assimilation to explain the increase in Sr isotope ratios (unpublished data).	Differences in origin of magmas and whether or not assimilation is involved.	Model based mostly on zircon data, zircon saturation thermometry and Zr-SiO_2 trend. Bulk assimilation (binary mixing calculation) of either 12% Ordovician sediments or 20% local S-type granite to explain the increase in $^{87}Sr/^{86}Sr$ from mafic to felsic samples, and the presence of minor zircon inheritance. Contribution of degree of partial melting of source to the geochemical variation not modelled.
Kemp *et al.* (2005) Cobargo model	Unspecified	Fractional crystallisation and in situ crystallisation[3]	Crystal-liquid mixtures[4]	Unspecified. No heterogeneity observed.	Differences in origin of magmas and whether or not assimilation is involved.	Model based mostly on zircon data, zircon saturation thermometry and Zr-SiO_2 trend. Crystallisation of a Zr-undersaturated parental magma creates a mushy zone (gabbros and diorites), with differentiated melt displaced to the top and centre of the magma body, eventually leading to Zr-saturation. Inefficient segregation of zircon-bearing crystal cargo from progressively fractionating melt produces trend in granites. Zr-rich sample is inferred to contain melt near Zr-saturation. This sample is estimated to have 30% melt, leading to an estimate of 460 ppm Zr (assuming $D_{Zr} = 0.1$) and 66 wt% SiO_2 (based on plag-cpx-opx-Fe-Ti oxide cumulus) in 870°C melt. Melt in granitic samples inferred to be cooler and lower in Zr than this melt, explaining moderated Zr-SiO_2 anti-correlation.

(Continued)

Table 1: Continued

Model	Origin of parental magma	Cause of linear trends	Physical state of granite magma	Cause of isotopic heterogeneity *within* suites	Cause of isotopic heterogeneity *between* suites	Model details
Kemp *et al.* (2007) mixing model	Mixing of mantle-derived basaltic magma with supracrustal material.[5]	Unspecified	Crystal-liquid mixtures	Inherent to parental magma being a mixture. Zircon Hf-O isotope arrays reflect various degrees of mixing.	Differences in proportions of the mixing endmembers; also possible variations in the isotopic composition of the crustal components.	Zircon Hf-O isotope arrays for each of three suites (Jindabyne, Why Worry and Cobargo) modelled using AFC model of DePaolo (1981). Using various mantle-derived and supracrustal mixing endmembers (the AFC primary magma and assimilant, respectively), up to approximately 25% supracrustal material for Cobargo, 40% for Jindabyne and 60% for Why Worry was inferred to be incorporated into the magmas forming the granites.

[1]Trends not necessarily strictly linear, but subtle curvature may be hidden by scatter in data; superimposed crystal accumulation and equilibration of melt-crystal mixtures bring trends closer to linearity.
[2]I-types are liquids based on Collins (1996) modelling, and S-types have minor crystal content (restite of the sedimentary endmember); but Collins (1998) re-emphasised the present of crystals in S-types and suggested I-types contained mafic clots of restitic or mixed origin.
[3]Linear trends in granitoids are extended to become curved and kinked by inclusion of spatially associated gabbros and diorites.
[4]Mafic samples (particularly gabbros and diorites) are mushes of cumulate minerals, and felsic samples represent crystal-liquid mixtures with increasing proportions of increasingly evolved melt.
[5]Mantle-derived material was favoured as the predominant source of the mafic magmas, but an infracrustal origin for them is admitted as possible. The supracrustal material could be (meta-)sedimentary rocks or S-type granites or partial melts derived therefrom.

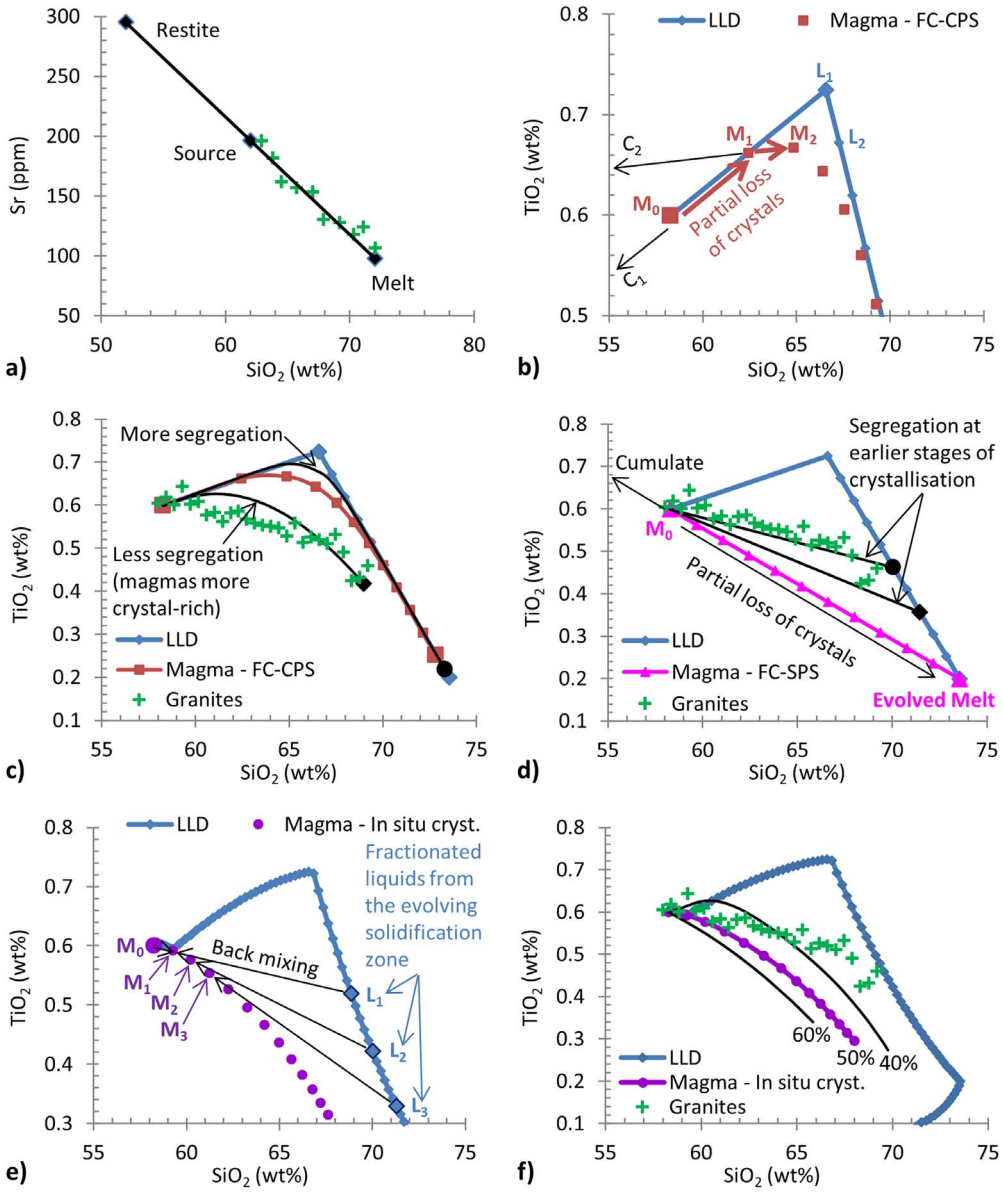

Fig. 1. a) Sr ppm vs. SiO_2 (wt%) for a hypothetical restite-controlled granite suite. Since the melt is derived from the source and the restite is the complementary component, all three and any magmas derived by melt-restite segregation (restite unmixing) will be collinear on all element-element plots. b) Illustration of fractional crystallisation with *concurrent* partial segregation (FC-CPS). As the parental magma (M_0) crystallises, its melt component evolves along the LLD. Partial loss of the crystal cargo C_1 from M_0 once the melt has reached L_1 moves the magma composition to M_1. After further crystallisation, the melt evolves to L_2 and the crystal cargo evolves to C_2, so further partial segregation shifts the magma to M_2. In this fashion FC-CPS produces the series of magma compositions shown. In c) this shown in relation to a hypothetical granite suite, and the thin lines bracketing the magma trend show alternatives for different degrees of melt-crystal segregation. Note that, for less segregation, the magma containing the most SiO_2-rich melt does not reach very high SiO_2 contents due to its relatively mafic crystal cargo. d) Illustration of fractional crystallisation with *subsequent* partial segregation (FC-SPS). For varying degrees of segregation occurring after crystallisation of the parental magma (M_0) has produced an evolved melt, magma compositions are linearly related, exactly analogous to restite unmixing. The slopes of the trends depend on how far along the LLD the melt evolved before segregation. e) For *in situ* crystallisation, the melt in the solidification zone evolves from M_0 along a LLD to L_1, some fraction of which is mixed back into the resident magma. Thus the parental magma (M_0) evolves to M_1, which becomes the new solidification zone composition. As the resident magma evolves, the composition of the fractionated liquid after a set degree of crystallisation will also evolve (this example assumes for simplicity that the iterations of resident magma have convergent LLDs, thus only one it plotted). In f) the magma evolution is shown relative to the same hypothetical granite suite as used in other plots. This example assumes 50% crystallisation in the solidification zone before back mixing of the fractionated liquid and retention of some melt in the solidification zone (10% of zone mass), and the thin lines bracketing the trend represent variations in the degree of crystallisation as marked (these trends are truncated at the first iteration for which the resident magma mass is <20% of initial mass).

variability and the common linear geochemical trends (Collins, 1996; Keay *et al.*, 1997; Collins, 1998; Healy *et al.*, 2004).

The three-component mixing model (Table 1), outlined in Collins (1996) and Keay *et al.* (1997), proposes that juvenile mantle-derived basaltic melts, Cambrian greenstone-derived melts and metasedimentary rocks (in the form of mid-crustal diatexites) mix in that order to produce a parent composition (Fig. 2b) that subsequently undergoes FC. For example, a tonalitic composition produced by mixing of

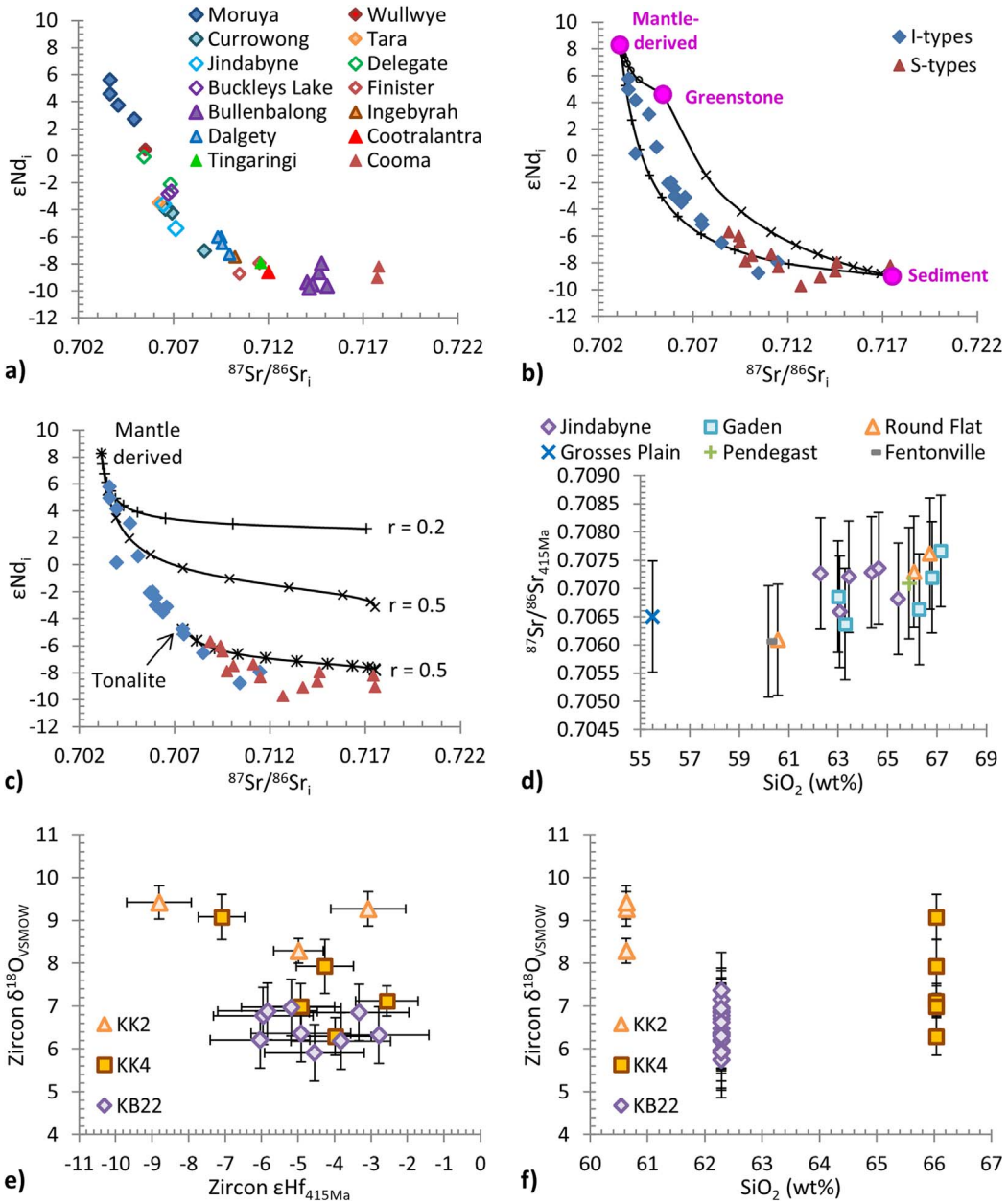

Fig. 2. a) Nd- and Sr-isotopic compositions of LFB granites, showing the clustering of data for each suite, with diamonds for I-types and triangles for S-types (Iles *et al.*, 2020). b) The Nd- and Sr-isotopic compositions of I- and S-type granites of the LFB are roughly contained within the field created by the mixing lines between the three labelled end-members of the three-component mixing model. (Chappell *et al.*, 1987; Collins, 1996; Keay *et al.*, 1997; Wyborn *et al.*, 2001). c) The same array plotted with AFC trends (DePaolo, 1981) involving assimilation of a sedimentary melt by a mantle-derived melt (upper two) and by a I-type tonalitic melt (lowest). Each trend is labelled with the ratio of assimilation to fractionation (where r is the ratio of the rates of assimilation and FC). Note that although the granite compositions are not accounted for by a mantle-derived primary melt (Keay *et al.*, 1997), an I-type primary melt that assimilates sediment could account for the Nd- and Sr-isotopic composition of the S-type granites. d) Bulk-rock Sr isotope composition vs. SiO_2 content for the different plutons of the Jindabyne Suite. Given the 2 s.e. uncertainties (reflecting reproducibility of sampling), there is no distinguishable correlation. e) Paired O and Hf isotope compositions of magmatic zircon from samples KK2 & KK4 (Round Flat pluton) and KK22 (Jindabyne pluton). f) Magmatic zircon O isotope composition vs. bulk-rock SiO_2 content for the same samples, showing partial overlap of $\delta^{18}O$ values. Note the decoupling of $\delta^{18}O$ values from the SiO_2 contents.

the first two components might be the parent magma of an I-type suite (such as Jindabyne and Moruya) or might further mix with a metasedimentary component to produce the parent magma of an S-type suite.

A natural possibility to consider is that the 'mixing' is, at least at some stage, accompanied by concurrent FC, as in AFC models. Fig. 2c illustrates the application of the AFC model of DePaolo (1981) to the generation of the LFB granite Sr-Nd isotope array (Keay *et al.*, 1997). That modelling does not encompass the role of assimilation once the proposed mixing process has generated the parental magmas. The three-component model does, however, admit the possibility that AFC could be involved locally in magma chambers to produce

within-pluton and within-suite geochemical variation (Collins, 1998). This would overprint the larger isotopic array, adding variation at the pluton to suite scale.

Regarding AFC in mixing models, Kemp *et al.* (2007) presented O-Hf isotope arrays in zircon populations in three I-type suites, suggesting mixing between mantle-derived and sedimentary end-members. In the presented model (Table 1), crystallisation and differentiation of basaltic magmas in the lower crust is accompanied by varying degrees of assimilation of buried supracrustal material. This model does not actually specify the degree to which the bulk geochemical variations within the pluton are generated by deep differentiation and hybridisation vs. emplacement-level crystallisation-differentiation, nor has the possibility to reconcile the model with all of the available data been tested. Investigation of the roles of FC and assimilation in the formation of the Jindabyne Suite as an example could shed light on this.

Fractional crystallisation and assimilation

Table 1 provides an overview of some important examples proposing FC, sometimes combined with concurrent assimilation (AFC), as a differentiation mechanism involved in the production of the geochemical trends of LFB granites (see also: Soesoo, 2000; Healy *et al.*, 2004). Note that the Jindabyne Suite is included among the models presented by Kemp *et al.* (2005); however, the models were based only upon Zr-SiO_2 relationships, rather than addressing all of the major element trends.

Common to some FC models are questionable assumptions surrounding phase stability and partition coefficients. In addressing the possible causes of linear variation on Harker diagrams, Wall *et al.* (1987) stated that 'Under certain circumstances, even pure Rayleigh fractionation can yield sensibly linear trends' (p. 740). Specific examples include Rayleigh fractionation models for the Jindabyne Suite (Wall *et al.*, 1987) and the Moruya Suite (Collins, 1996). Such models presuppose that a particular mineral assemblage would in fact crystallise from the parental liquid *and* would continue to crystallise without any major change as the liquid evolves through a relatively wide range of compositions (e.g. ~56 to 67 wt% SiO_2) without consideration of phase equilibria or the thermal evolution of the system to show that this is actually plausible. The introduction of a new mineral to the liquidus assemblage or progressive changes in the phase proportions and partitioning behaviour would lead to FC trends with distinct curvature and inflection points that could not be described as 'sensibly linear'. Given that such modelling was used as justification by Collins (1996) for FC being appropriate generally for producing linear trends in LFB granites, as part of the three-component mixing model, it is important these ideas be tested.

To test this idea with respect to one group of granites, it is necessary to consider the possible ways that crystallisation and assimilation processes could produce a set of related granite samples. Fractional crystallisation with perfect segregation of cumulates would produce a series of melt compositions and a corresponding series of instantaneous cumulates. In this way the LFB granite trends could represent liquid lines of descent (LLDs), the granite samples possibly representing melts tapped from a differentiating magma chamber at depth (Figs 3 and 4). Modelling the trends as LLDs has commonly been used in previous research in the LFB (e.g. Wall *et al.*, 1987; Collins, 1996) and worldwide (e.g. Jagoutz, 2010); therefore, this is one pre-existing hypothesis that should be tested.

Alternatively, the granites may represent a series of cumulates complementary to a LLD, with limited trapped melt. Under conditions of perfect segregation, this would be expected to form layered or zoned plutons, which are not observed. Instead, the granites might represent crystal-bearing magmas produced by FC with incomplete segregation of crystals (Fig. 4a). This idea encompasses a variety of conceptual models, which might still be viewed as fractional rather than equilibrium crystallisation if chemical isolation of melt from crystals is achieved through crystal zoning (for variations on this idea see: Hertogen & Mareels, 2016; Pupier *et al.*, 2008). If incomplete segregation of crystals is concurrent with the fractional crystallisation of the melt, the granites would represent mixtures between the LLD and a series of aggregated cumulate compositions. This might be called fractional crystallisation with concurrent partial segregation (FC-CPS), and is central to the model presented by Kemp *et al.* (2005) for the Cobargo Suite (Table 1). An example of such a trend is shown in Figs 1b–c and 4a. As illustrated, if the LLD has a sharp inflection point on a bivariate element plot the magma evolution trend will be curved: relatively subtly if only minor segregation occurs, but increasingly dramatically and approaching the LLD the more complete is the melt-crystal segregation. The generation of linear or near-linear trends in this way would, therefore, depend on the extent of deviation from linearity in the LLD and the amount of crystal retention. It should also be noted that compositional range of the magmas will be limited by the degree of segregation.

If, alternatively, varying degrees of segregation occur only after evolution of the melt by FC, magmas would vary linearly between the evolved melt and a crystal-rich composition equivalent to the parental liquid, in a manner analogous to restite unmixing (Fig.e 4a). This could be termed fractional crystallisation with subsequent partial segregation (FC-SPS). Fig. 1d illustrates that, in this case, the shape of the LLD would not be imparted upon the magma trend, but the point along the LLD at which segregation occurs would control the slope of the trend. This idea bears some similarity to the model of McCarthy & Robb (1978).

For AFC regimes in which the assimilant is partial melt of the wallrock (WR), the relationships between the LLD and trends created by different forms of liquid-crystal segregation would be similar to the relationships discussed for FC alone, with a few exceptions. For AFC-SPS, the crystal-rich end of the trend would change position for an AFC regime compared to FC-SPS, because the addition of WR melt to the magma alters the bulk composition of the system. The overall effect upon the magma trend for AFC-CPS compared to FC-CPS, however, will be subtle because the change in bulk composition due to WR melt assimilation is incremental, while the essential differentiation mechanism is the same for both. Thus, a modelling approach that constrains LLDs and the complementary cumulate compositions for FC and AFC processes can be employed to assess the capability of FC (±assimilation) to produce linear trends in granites whether the granites represent a series of liquids or mixtures of crystals and melt. A more complex variation of AFC would be one in which both melt and solid components are assimilated by the magma. This would place the magma trend between the bulk composition of the WR and the LLD based on the assimilation of only melt.

The evolution of the resident magma for *in situ* crystallisation involves progressively mixing compositions along an LLD with one iteration of the resident magma to produce the next (Figs 1 and 4b). As illustrated, this is *quantitatively* similar to partially segregating the crystals of one magma batch from the respective melt (a composition along an LLD). Since the evolution of the resident magma causes progressive changes in the LLDs followed in the advancing crystallisation

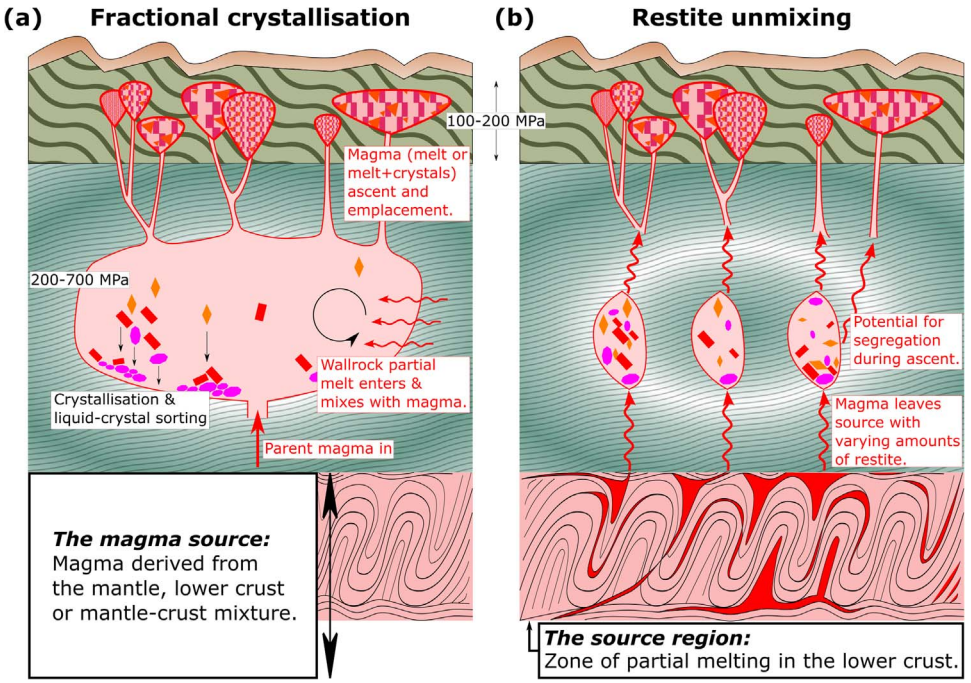

Fig. 3. Crustal schematics for magma diversification driven either by crystallisation-differentiation or melting and segregation. a) Illustration magma evolution driven by AFC in a magma chamber below the emplacement level of the granite plutons. The indicated chamber pressures reflect the possible range, constrained from observation. The emplacement pressure range reflects the range of Jindabyne Suite amphibole geobarometer estimates. Different authors (see main text) have provided various suggestions for the source of the parental magma. The specifics of crystallisation and liquid-crystal sorting within the magma chamber are explored in Fig. 4. b) Illustration of how the restite model could produce granite plutons via melting of the lower crust, segregation of magmas bearing residual crystals (restite), magma ascent (with possible unmixing), and emplacement of magma with varying proportions of melt and the restite assemblage. Schematics are not to scale.

zone, the composition of the fractionated liquid back-mixed into the resident magma would not necessarily be constant as Nishimura & Yanagi (2000) assumed. Rather, the slight but progressive shifts in resident magma composition may result in a range of broadly similar felsic compositions after equal degrees of fractionation in the crystallisation zone (Zhao *et al.*, 2018). Assimilation is not usually envisaged in *in situ* crystallisation models because solidification of the margin of the magma chamber would close the crystallisation zone to outside input.

BACKGROUND AND INTRODUCTION TO THE JINDABYNE SUITE

Geological background

The LFB and NEFB are part of the Tasman Orogen of southeastern Australia (Fig. 5). The LFB consists of a Cambrian-Ordovician basement; Ordovician to Silurian turbidites and broadly contemporaneous volcanic belts (mostly shoshonitic); Devonian to Early Carboniferous limestones and clastic rocks; and, elongated belts of granitoid bodies and related felsic volcanic rocks formed during Silurian-Early Devonian, Late Devonian and Carboniferous magmatic pulses (Chappell, 1984; White & Chappell, 1988; Chappell & White, 1992; Fergusson & Coney, 1992; Wyborn, 1992; Gray & Foster, 2004; Iles *et al.*, 2020).

The granites of the Kosciusko and Berridale batholiths, where the contrast between I- and S-type granites is marked, are some of the most extensively studied granitoids of the LFB (White *et al.*, 1976; White *et al.*, 1977; Hine *et al.*, 1978; Williams *et al.*, 1983; Chappell, 1984; Gray, 1984; Whalen & Chappell, 1988; White & Chappell, 1988; Chen *et al.*, 1989; Chen *et al.*, 1991; Collins, 1996; Sha & Chappell, 1999; Chappell & White, 2001; Gray & Kemp, 2009). These locations were the basis of a series of investigations into the H, O, Sr, Pb and Nd isotope characteristics of I- and S-type granites in the LFB (O'Neil & Chappell, 1977; McCulloch & Chappell, 1982; McCulloch & Woodhead, 1993).

An overview of the petrographic and geochemical characteristics of the granites (*sensu lato*) of the Kosciusko-Berridale region (including the Jindabyne Suite) was provided by Iles *et al.* (2020), but some salient details are highlighted here. The I-type suites include biotite granites and hornblende granites and tonalites (*sensu stricto*), some of which contain minor inherited zircon (Williams *et al.*, 1983; Williams, 1992). All of the granites (*sensu lato*) contain mafic microgranular/microgranitoid enclaves as well as hornfelsic xenoliths (which are restricted to the pluton margins and demonstrably represent country-rock), but the I-type granites do not otherwise contain metasedimentary enclaves (Chen *et al.*, 1989; Chen & Williams, 1990; Chen *et al.*, 1991).

In addition to the curved array formed by LFB granite bulk-rock samples in Sr-Nd isotope space (Fig. 2a; Keay *et al.*, 1997; McCulloch & Chappell, 1982), Iles *et al.* (2020) demonstrated a corresponding linear array of bulk-rock Nd and Hf isotope compositions. These data exhibit a general progression from mantle-like compositions, through the I-type then S-type granites towards evolved, sediment-like compositions in Sr-Nd-Hf isotope space, with minor overlap between the two granite types. That study also showed that many of the examined granites (particularly the I-types) record a discrepancy between the Hf isotope compositions of magmatic zircons and of

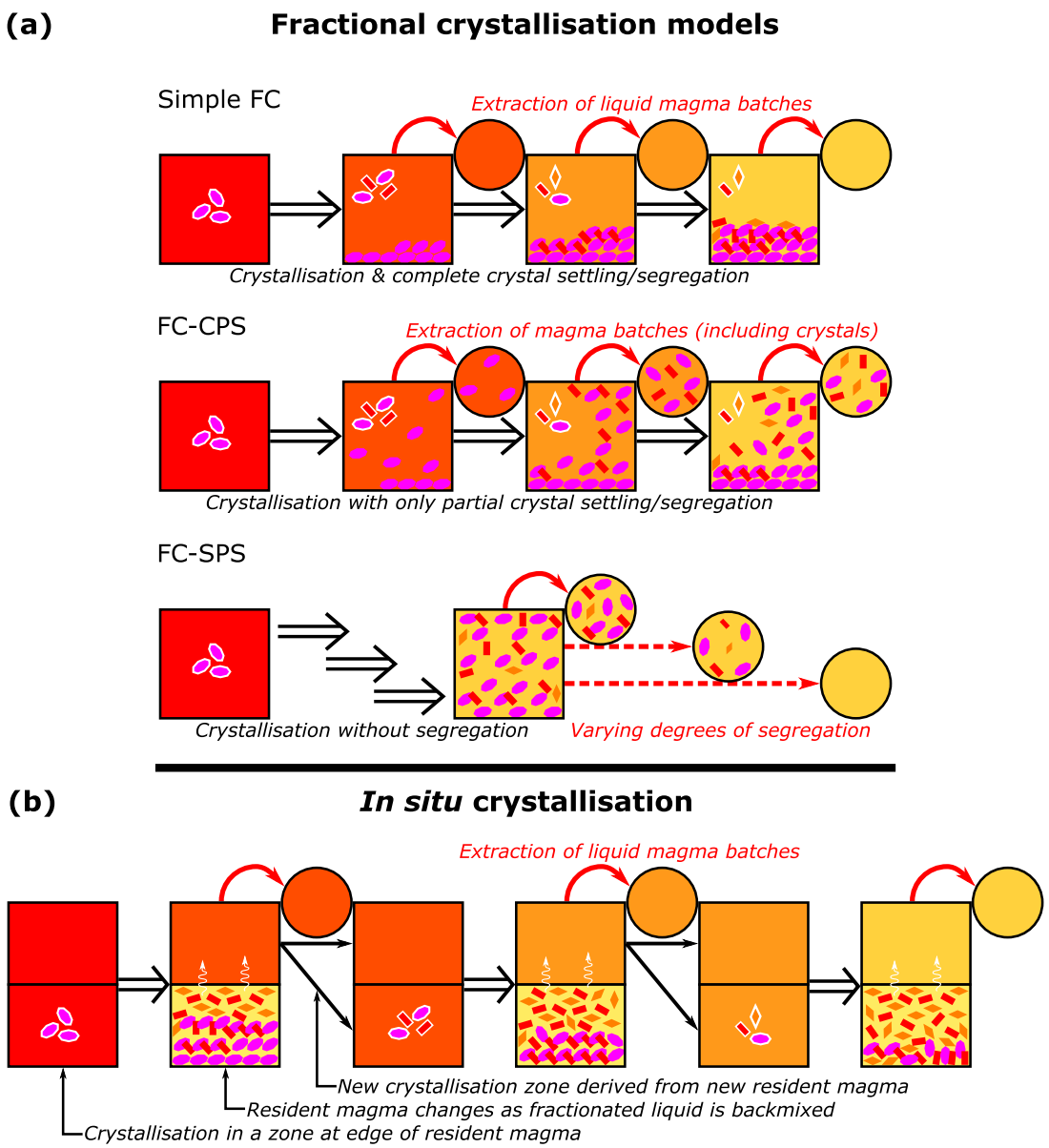

Fig. 4. Schematics representing the evolution of the magma via fractionation crystallisation-driven mechanisms. a) Three forms of FC, of the same parental magma. From left to right each box shows the different melts and the different liquidus assemblage (shapes with an outline), along with the cumulate pile at the bottom. Circles above boxes represent the sort of magma batch that would be extracted from each FC stage. 'Simple FC' illustrates production of liquid batches along a liquid line of descent; 'FC-CPS' illustrates the same evolution with only partial melt-crystal segregation, resulting in crystal-bearing batches; and, in 'FC-SPS', the magma progresses to the final stage without any segregation, but segregation/unmixing occurs in the extracted batches. Although not illustrated, melt could be assimilated into the magma, altering its composition. b) The same parental magma, undergoing *in situ* crystallisation. At each stage the upper portion of the boxes represent the resident magma, and the lower portion the crystallisation zone. This zone in FC-driven, producing a evolved melt, some of which is mixed back into the resident magma. The system progresses by creating new crystallisation zones from the new resident magma, from which liquid magma is extracted.

their host bulk-rocks. Although this was deemed to be consistent with a restite model origin for the granites, the data *do* permit a mixing origin for the granite magmas. Indeed, regarding the interpretation of the isotopic data, Iles *et al.* (2020) suggested that one of the problems with mixing models (such as those discussed above) was the questionable plausibility of FC as a mechanism for the production of linear within-suite trends; therefore, the restite model interpretation was preferred. The investigation of FC here is, therefore, relevant for possible alternative explorations of the isotope data.

The Jindabyne Suite

The Jindabyne Suite is a collection of nine geographically, petrographically and chemically associated lithological units (for some units the plutons are probably composites, although clear intrusive boundaries are not mapped, but other units consist of just 1–2 neighbouring plutons), most outcropping in the Kosciusko Batholith (Fig. 5). Descriptions of these lithological units from White *et al.* (1977), Owen & Wyborn (1979) and White & Chappell (1989) have been compiled in the Supplementary Material and summarised here.

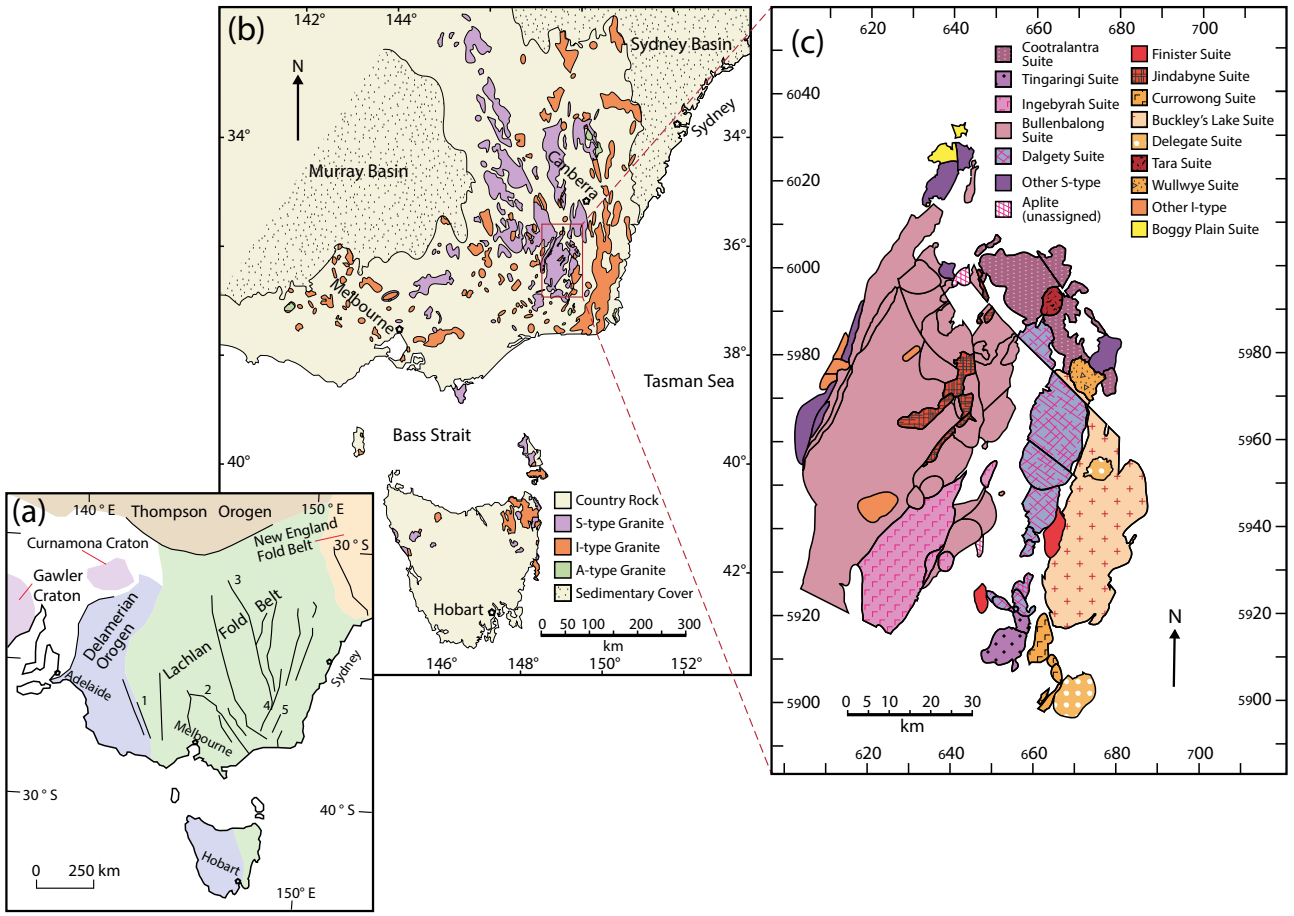

Fig. 5. Geological maps of southeastern Australia, including the setting for the Jindabyne Suite from Iles *et al.* (2020). a) Map of the Tasmanides, including the Lachlan Fold Belt (LFB), which is divided into the Western, Central and Eastern Lachlan by the Stawell-Ararat Fault Zone (1), the Governor Fault Zone (2) and the Gilmore Fault Zone (3). The Indi Fault (4) bounds the western side of the Kosciuszko Batholith and the Yalmy Fault (5) coincides with the I-S line that runs through the Berridale Batholith. b) Map of the LFB, showing the distribution of granitoids. c) Map of the Kosciuszko and Berridale batholiths, showing the locations of the Jindabyne Suite plutons. I-type plutons are listed on the right and S-types on the left in the legend.

Samples of the Jindabyne Suite exhibit ~46–57% pearly white plagioclase grains with corroded, highly calcic cores (An_{80}) surrounded by mantles of An_{65} to An_{25} (mostly An_{40} to An_{30}). Samples may differ in biotite and hornblende abundance (~9–21% and ~0–20%, respectively) and grainsize, but these phases are otherwise petrographically similar from sample to sample. In many examples hornblende crystals occasionally contain relict clinopyroxene or colourless amphibole pseudomorphs after pyroxene. Orthoclase is rare (almost all samples are tonalites) and is interstitial. Quartz is often interstitial to plagioclase, but in some cases is found as inclusions in calcic plagioclase cores and in others is found as large (4 mm wide) patches enclosing plagioclase. Magnetite, apatite and zircon are found as accessory phases in all samples, whereas the occurrence of allanite varies from absent or rare in most cases to being present as crystals up to 1 mm long in one unit.

The major element data for the suite are plotted in Harker diagrams in Fig. 6, illustrating that the linear geochemical trends of the suite as a whole are mimicked by the trends for the individual lithological units represented by four or more samples (Jindabyne, Round Flat and Gaden). Similarly, for any bivariate element plot (e.g. Fe_2O_3 vs. SiO_2 or CaO vs. Na_2O) the degree of scatter within the suite as a whole is reflected by scatter in the data for individual lithological units. Select trace elements are plotted against SiO_2 in Fig. 7, demonstrating similar geochemical variation to that displayed for major element oxides.

The H_2O contents measured in the samples show a decrease from ~2 to ~1 wt% (total water) with increasing SiO_2 contents (Fig. 6h). Although this is suggestive of fractionation of hydrous mineral phases (such as the observed biotite and amphibole), upwards of 50% of the fractionating assemblage would need to be biotite (with ~4 wt% H_2O) to account for the trend, and amphibole (with ~2 wt% H_2O) would not be capable of producing the trend even if it occupied 100% of the assemblage. Thus, we do not regard the H_2O-SiO_2 trend as a product of magmatic fractionation. Furthermore, two observations suggest that the anhydrous phases dominated the fractionating assemblage and that the hydrous phases are late-stage magmatic products: (1) the textural relationships between amphibole and pyroxene in the samples are consistent with a reaction relationship as described by White (2002), and (2) where LFB I- and S-type granites can be associated with volcanic equivalents, the phenocrysts on the volcanic units are more anhydrous (e.g. quartz+orthopyroxene+clinopyroxene+plagioclase with minor biotite and hornblende in I-types) than the granite mineral assemblage (quartz+biotite+hornblende+plagioclase+K-feldspar), which implies that the growth of biotite and amphibole is a feature developed during the solidification of granite plutons (Chappell

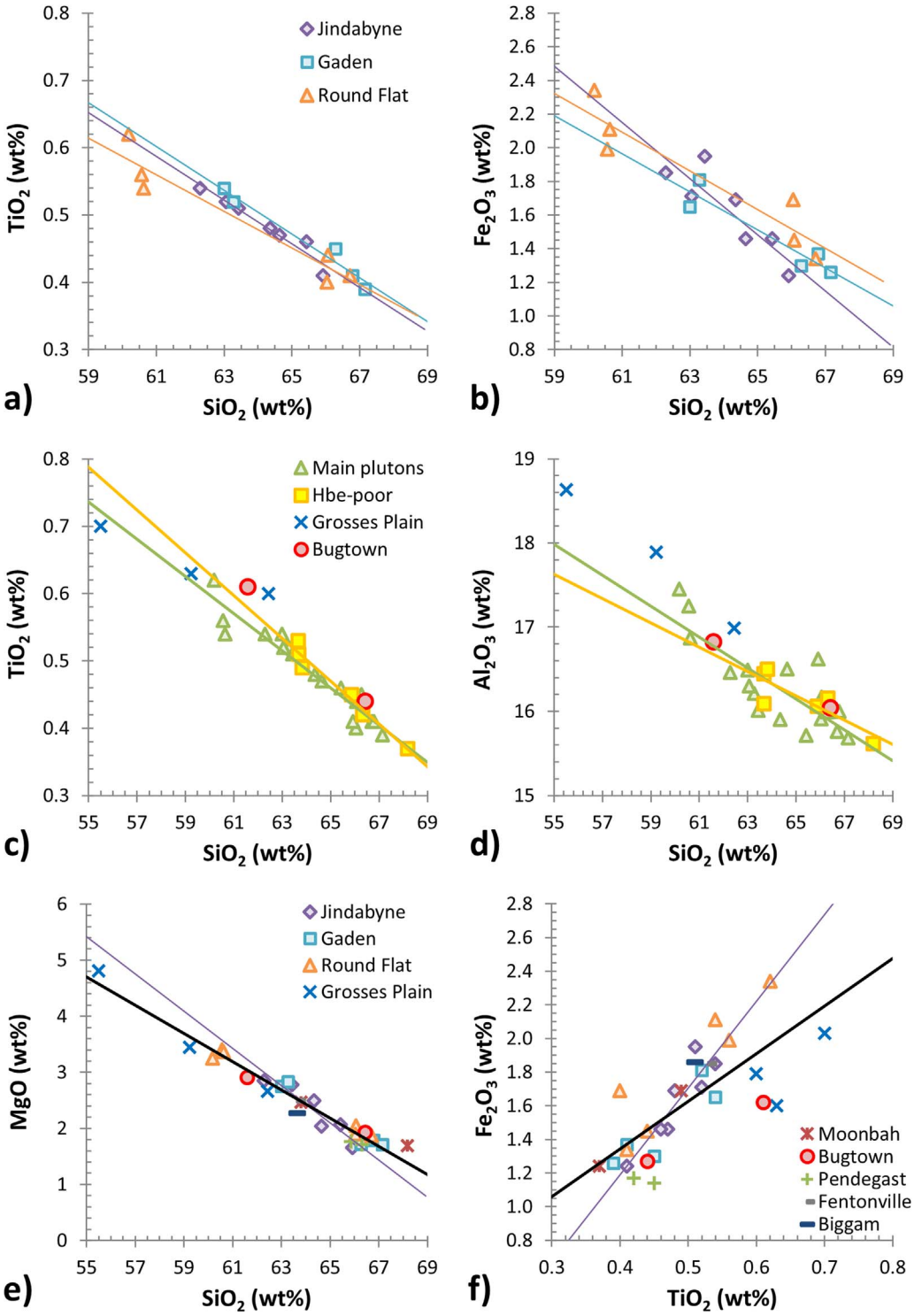

Fig. 6. Harker diagrams representing the major element variations within and between the plutons of the Jindabyne Suite. The data have been grouped in different ways to illustrate the consistency of the geochemical character of the different units that constitute the suite and how they form the overall Jindabyne Suite trends. In a) and b) just the three most sampled units have been plotted. Note that linear variation is evident at the level of individual units; furthermore, the variation in each is part of a wider trend. In other plots these three (Jindabyne, Gaden and Round Flat) have been groups as the 'main plutons'. Those units that have many petrographic features in common with these but are exclusively represented by hornblende-poor samples have been grouped separately, while the mafic Grosses Plain and petrographically variable Bugtown plutons have been plotted individually. In this way it is clear from c–d) that the trend defined in the most variable and well-sampled plutons (main plutons) is matched by other groups of petrographically related plutons, hence their grouping into the Jindabyne Suite. Plots e–h) show all units individually, demonstrating their coherency: where a trend is clear (e–f), the trend through the Jindabyne pluton (thin line), for example, is similar to the trend line for the suite as a whole (thick black line); for trends such as P_2O_5 vs. SiO_2 (g) where there is considerable scatter, this scatter is also represented within each unit. For i–l) the samples are grouped as in c), and again the consistency of the variations is clear.

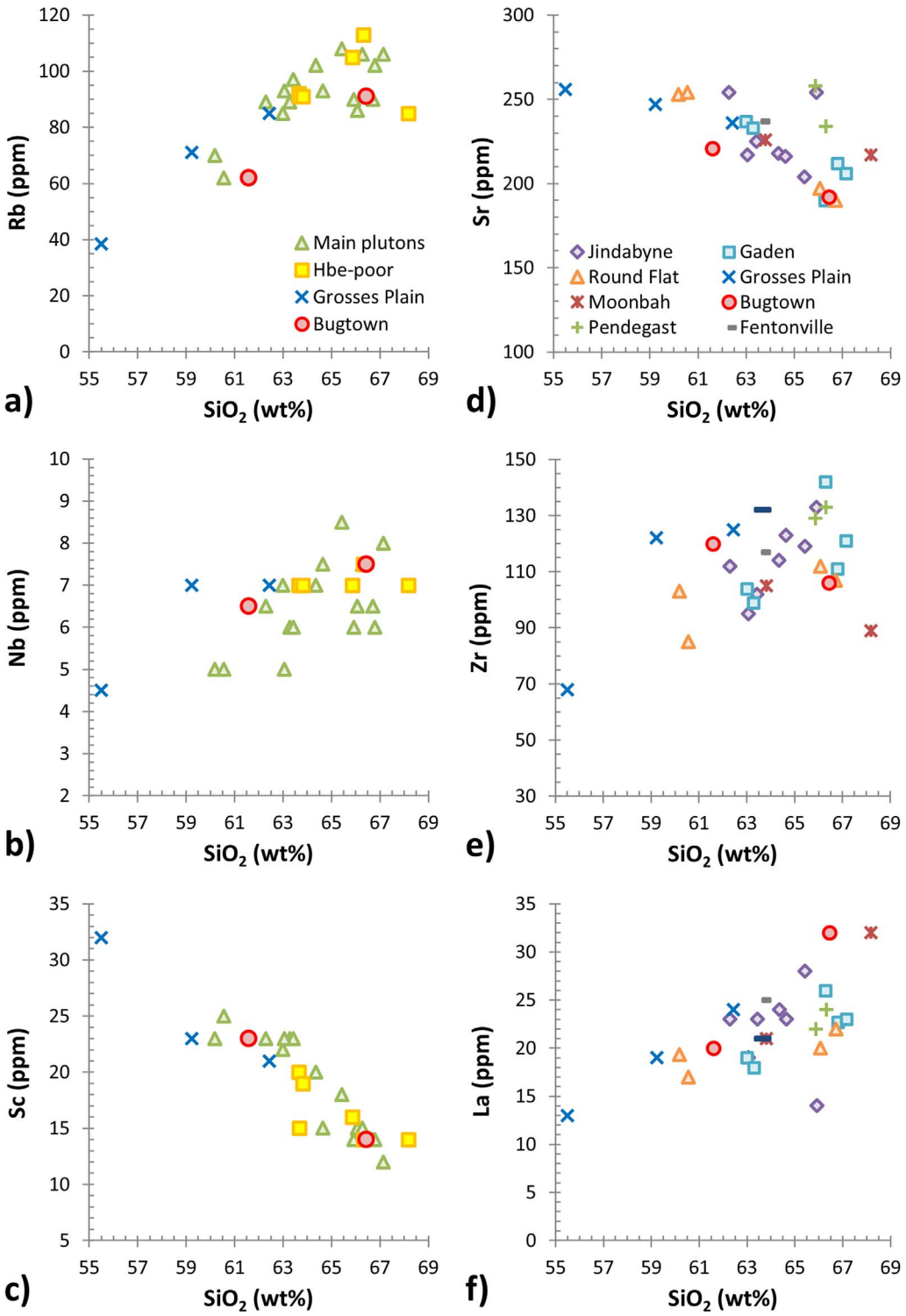

Fig. 7. Select trace elements plotted against SiO_2 for bulk-rock samples of the Jindabyne Suite, with groupings as explained in Fig. 6. a–c) Comparison of the trends formed by the dominant units (main plutons) with the variations in exclusively hornblende-poor units, the mafic Grosses Plain pluton and the zoned Bugtown pluton. d–f) Show the variations within individual units. As for the major elements, the trace elements show linear variation with SiO_2 content across the suite, although there is greater scatter for the trace element; and the overlapping variations in individual units build the broader trends of the Jindabyne Suite.

& White, 1992). These observations suggest that amphibole thermobarometry (explored below) would reflect emplacement conditions.

There are several studies that investigated isotopic data from the Jindabyne Suite, through both *in situ* targeting of zircon and bulk-rock sampling (Compston & Chappell, 1979; McCulloch &

Chappell, 1982; Kemp *et al.*, 2005; Belousova *et al.*, 2006; Kemp *et al.*, 2007; Ickert & Williams, 2011; Iles *et al.*, 2020). A detailed assessment of the combined data sets is provided in the Supplementary Material and a summary of key points follows.

The U–Pb zircon geochronological studies (Kemp *et al.*, 2005; Belousova *et al.*, 2006; Ickert & Williams, 2011) show a spread of ages (sample mean ages of ~416–424 Ma) both within and between plutons, suggesting diachroneity in the Jindabyne Suite and a long magmatic history involved in the generation, differentiation and crystallisation of the suite. This is consistent with incremental intrusion of magma batches produced by processes occurring at depth rather than diversification of a common parental magma via *in situ* crystallisation in each pluton.

Combining the data from Compston & Chappell (1979), McCulloch & Chappell (1982) and Iles *et al.* (2020), the $^{87}Sr/^{86}Sr_{415Ma}$ of Jindabyne Suite samples range from 0.70606 to 0.70767. Although a somewhat scattered trend of increasing $^{87}Sr/^{86}Sr_{415Ma}$ with increasing SiO_2 might be suggested, poor reproducibility makes the presence of a correlation ambiguous (Fig. 2d). Thus, the Sr isotope compositions of individual samples are, in fact, indistinguishable (weighted mean $^{87}Sr/^{86}Sr_{415Ma} = 0.70693 \pm 0.00024$, 2σ, MSWD = 1.01, N = 17). Similarly, given the reproducibility, four samples with Nd isotope compositions from $\varepsilon Nd_{415Ma} \approx -3.8$ to -5.8 (relative to the CHUR composition of Jacobsen & Wasserburg, 1980) are indistinguishable.

When considering the combination of the zircon Hf and O isotope data from Kemp *et al.* (2007) and from Iles *et al.* (2020), we have examined only the data for which O and Hf isotope analyses can be matched to U–Pb age determinations consistent with the magmatic ages noted above for the samples, so that we can be confident that the compositional data reflect truly magmatic (not inherited or reset) zircon domains that capture real variability in the melt component of these granites. As shown in Fig. 2e, the different plutons (Round Flat and Jindabyne) are broadly similar isotopically. Analysis of the data (Supplementary Material) reveals no statistically significant O-Hf isotope correlation in the data at the sample and suite level. Furthermore, although there is a slight difference between the O isotope compositions of these zircon populations, their means do not correlate with SiO_2 (Fig. 2f). Thus, the magmatic zircon O-Hf isotopic diversity is not directly related to the bulk-rock major element variations.

MODELLING METHODS

The Magma Chamber Simulator

Overview of the MCS

The MCS programme (Bohrson *et al.*, 2014; Bohrson *et al.*, 2020) tracks the geochemical, petrological and thermal evolution of a composite system consisting of a magma body (resident melt ±crystals ±fluids), cumulate reservoir, wallrock (WR) and a set of recharge magma reservoirs using the MELTS family of phase-equilibria equations (Ghiorso, 1985; Ghiorso & Sack, 1995; Gualda *et al.*, 2012). Cooling and crystallisation of the magma body delivers enthalpy to the WR, heating and (potentially) partially melting it. Melt produced in the WR may contaminate the magma body (Fig. 3), which may also receive thermal and material input via magma recharge. Additionally, by using the appropriate composition, bulk assimilation of WR can be simulated as 'recharge' (i.e. stoping) events.

The main input parameters of MCS are the subsystem (magma, WR, recharge magmas) major and minor element compositions and oxygen fugacity, subsystem initial temperatures, WR and recharge masses (relative to 100 units of initial magma mass), the WR melt fraction above which WR melt will be assimilated (critical melt fraction), the timing of recharge events, and the universal system pressure. The progress variable of MCS is the resident magma temperature. A user-defined temperature decrement causes equilibrium crystallisation of the resident magma and delivers heat to the WR – at the end of the decrement step, the formed cumulates are fractionated into a cumulate reservoir. These steps are interrupted by possible additions of WR partial melts, stoped blocks, or recharge magma into the resident magma subsystem. For more details on the MCS input, computational operations, and output, see Bohrson *et al.* (2020).

Following completion of an MCS run, it is possible to model the corresponding trace element and isotopic evolution, utilising the phases, masses and subsystem temperatures of the MCS output file and used-defined initial compositions and partition coefficients. Details of the trace element and isotope computation are provided in Heinonen *et al.* (2020).

Modelling limitations

The MCS programme inherits the limitations of whichever MELTS version (rhyolite-MELTS 1.0.2, 1.1.0 or 1.2.0, or pMELTS) is used for a particular run. Accordingly, some phases and subsystem compositions are problematic. For example, very hydrous systems with extensive fractionation of phases such as biotite or hornblende are not handled optimally by MELTS (Gualda *et al.*, 2012; Ghiorso & Gualda, 2015; Bohrson *et al.*, 2020). This is discussed later in relation to models presented in this study. Some phases are not modelled by MELTS, and only a limited set of accessory phases (e.g. apatite and oxides) are included in the MELTS algorithms (Ghiorso & Sack, 1995). Although several accessory phases are critical for specific sets of trace elements (e.g. Zr, Hf and HREE for zircon, and LREE for monazite), these phases have little bearing on the major element evolution of a magmatic system. In I-type granites monazite is rarely observed, whereas apatite is ubiquitous, but both phases might be relevant for a metasedimentary WR. There is a wealth of major and trace element information that can be explored with MCS without considering these accessory phases. The limitations resulting from what MELTS can model are important in guiding what aspects of the compositional evolution can be reliably examined through MCS, but they do not mean that MCS will entirely fail to model a system that contains an unhandled accessory phase.

The capability of the modelling presented herein to reflect natural systems is also constrained by two aspects of the way assimilation is handled in the MCS: equilibrium melting in the WR and mass transfer from WR to magma. Melting in the WR is assumed to occur at equilibrium at each temperature step in the models. Whether this actually applies for our case study is difficult to assess because, if assimilation is involved in the production of the Jindabyne Suite, it must have occurred below the current exposure level of the plutons, since their country rocks do not show evidence of partial melting (they can be termed 'contact aureole' rather than 'regional aureole' granites; White & Chappell, 1988). The possibility that WR partial melting was affected by disequilibrium processes cannot currently be addressed with the MCS; therefore, the equilibrium assumption is taken as a simplification necessary to conduct extensive modelling of AFC processes with thermodynamic constraints. Additionally, the MCS handles assimilation as a one-way mass exchange into the magma: either WR blocks are stoped and completely mixed into the magma, or WR melt is advected from the WR into the magma. Our

modelling cannot, therefore, explore AFC involving two-way diffusional transfer of elements, which London *et al.* (2012) demonstrated can occur (particularly for alkalis and H) when a granitoid melt is in contact with WR containing interconnected partial melt.

Approach

Taking the Jindabyne Suite as a case study, this investigation has used the MCS to model magmas undergoing FC both with and without concurrent assimilation, focusing particularly on how closely the simulations match the linear major element trends. These models have also been extended to more complex variations. Although we present a single case study, the process of extensively exploring diverse FC (±assimilation) scenarios can provide insight into the formation of other granitoid suites with similar trends.

While the involvement of open-system processing has been evoked in various ways for the generation of LFB granitoids, we have not assumed assimilation necessarily should be included in simulations of the Jindabyne Suite evolution for two reasons: (1) although the data demonstrate isotopic heterogeneity within the Jindabyne Suite, they do not definitively show an isotopic evolution that would necessitate open-system behaviour coupled to the generation of major element variability (Fig. 2), and (2) the existing quantitative models for the geochemical variations in these granitoids (Table 1) focus on FC without assimilation. Thus, the modelling presented here starts with FC alone and considers assimilation as an option that could allow the trends to be better modelled.

The possibility of producing the observed trends as LLDs was tested first. This involved combining sets of sensitivity studies of certain input parameters with iterative attempts to obtain the closest possible fit to the Jindabyne Suite data. The best-fit FC and AFC models were extended to include select trace elements and the radiogenic isotope systems, providing a test of whether the models that explain the major element evolution are consistent with the trace element and isotope data. A large extent of the modelling focused on the trends in liquid compositions because the input parameter space that can be tested in MCS when assimilation is included is extensive and because the LLD is a critical constraint on the sorts of trends that partial segregation models can produce. In order to assess the plausibility of FC-CPS, FC-SPS and *in situ* crystallisation to model the trends, criteria for the associated LLDs must first be established. This firstly allows the existing set of simulations to be examined for potential candidates upon which to base these alternative models, and secondly establishes what would be required of additional simulations, the most suitable of which were also extended to trace element modelling.

By combining the MCS output information about magma compositions and the masses of fractionated phases, it is possible to calculate the instantaneous and aggregated cumulate compositions for every step of the simulation, and thus model FC-CPS and FC-SPS (±assimilation). For differentiation with subsequent partial crystal segregation (FC-SPS), a binary mixing line between the initial magma and some evolved magma could model either all or part of the bulk-rock variation; the aggregate cumulate composition determines the extreme melt-depleted end-member to which the mixing/unmixing line extends, potentially delineating accumulative bulk-rock samples; and the MCS phase composition output data describe the sort of mineral compositions that would constitute a portion of all samples in a suite. For differentiation with concurrent partial crystal segregation (FC-CPS or AFC-CPS), the resident magma and cumulate composition and mass outputs can be combined in different ways to produce a crystal-bearing magma evolution to correspond to bulk-rock granite samples.

Given the way fractional crystallisation ± assimilation with subsequent partial segregation (FC-SPS, AFC-SPS) functions (see above and Fig. 1d), the criteria for the LLD for FC-SPS are: (1) the magma initial composition is on the linear regression of the data (presumably near the mafic end, but potentially an intermediate composition), and (2) the LLD reaches a point on the linear regression at least as felsic as the most felsic sample. With the involvement of assimilation, the first criterion is modified to be that the mixture of initial composition plus aggregated mass of assimilated WR melt is on the linear regression. For fractional crystallisation ± assimilation with *concurrent* partial segregation (FC-CPS, AFC-CPS) strictly linear trends would not arise unless the LLD were also linear (Fig. 1b–c), but sufficiently near linear trends, matching the data, could be formed if the following criteria were met: (1) the magma initial composition is near the mafic end of the observed trends, (2) the LLD evolves to compositions *near* the linear regression at SiO_2 contents at least as high as the most felsic sample, and (3) the LLD does not deviate greatly from the observed trends at any of the intermediate compositions.

The criteria for suitable LLDs under an *in situ* crystallisation model are similar to those for FC with partial segregation, due to the similarity between their LLD-magma relationships (Fig. 1). Given likely variations in fractionated liquid composition, LLDs would need to meet the criteria: (1) the magma initial composition is on the linear regression of the data (presumably near the mafic end, but potentially an intermediate composition), and (2) the LLD evolves to compositions *near* the linear regression at SiO_2 contents at least as high as the most felsic sample. The criteria for LLD under FC-CPS would apply if only minimally fractionated melt were back-mixed from the crystallisation zone into the resident magma.

Lastly, the effect of bulk assimilation or entrainment of a portion of WR restite with assimilated melt can be assessed by the relationship between LLDs for AFC models and the WR bulk composition, and further investigated with the assimilation by stoping function of MCS. This along with the approach outlined above allow diverse variations of FC-controlled magmatic differentiation to be examined as potential models for the Jindabyne Suite.

MODEL RESULTS

Temperature, pressure and volatile contents

The initial temperature of the magma is constrained in each model to the liquidus temperature for the composition at the model's pressure, according to the thermodynamic calculations of MELTS. It is possible to consider the starting magma at a lower temperature, but such a magma would, by definition, be liquid-crystal mixtures. In MCS, magmas initially below their liquidus temperature automatically form that crystal component as the first 'cumulates'. The subsequent partial segregation models capture differentiation of crystal bearing magmas at temperatures below the liquidus.

The relevant pressures for testing the models can be loosely constrained by considering a few observations. The spread of ages for Jindabyne samples point to growth of the various plutons of the suite by injection of different magma batches over time, implying magma diversification below emplacement level. Additionally, the consistency of within-pluton variation with the variation of the suite as a whole for a series of plutons of diverse sizes would be more consistent with the main form of differentiation occurring at depth, than with each different pluton undergoing its own differentiation yet achieving conformity to an overall Jindabyne Suite trend (see introductory section and Figs 6 and 7). Given the observed

amphiboles are assumed to have formed late in the crystallisation sequence and likely at emplacement level (as discussed above), amphibole geobarometry can provide a lower limit on the pressure for modelling (A)FC.

The supplementary material of Whalen & Chappell (1988) provides major element compositions for amphibole grain domains from four Jindabyne Suite samples. Grain average compositions are provided in Table 2. Most of these classify as magnesiohornblende but one grain is cummingtonite. Application of the Ridolfi (2021) thermobarometer to magnesiohornblende yields pressures and temperatures that are consistent within individual grains and samples given the uncertainties (12%, and 22°C, respectively, 1σ). The average grain temperatures range from 758 ± 22 to 805 ± 16°C, while the average grain pressures range from 110 ± 13 to 166 ± 20 MPa. The Al^{VI} amphibole geobarometer of Krawczynski *et al.* (2012) yields large variations in pressure estimates within-grain and within-sample (consistent with the 142 MPa uncertainty). Nevertheless, the grain average pressure estimates are similar (140–230 MPa, and an outlier at 680 MPa).

These pressure determinations are consistent with the estimated emplacement depth for other Siluro-Devonian granites in the region (e.g. 100 MPa, 4–5 km for the Deddick Granodiorite; Maas *et al.*, 1997). Furthermore, the pressure estimates for crustal zones envisaged by Collins (1998) for the three-component mixing model for the LFB granites would place Jindabyne magma formation between ~20 km (600 MPa) and ~ 30 km (1000 MPa), providing an approximate maximum pressure for modelling magma differentiation. Being emplacement pressures, the 110–166 MPa for Jindabyne amphiboles would be an approximate minimum pressure for modelling. The results of sensitivity tests (see below) ultimately lead to models between 150 and 700 MPa (mostly 300–500 MPa).

Given the likelihood that the measured water contents of the samples do not represent original concentrations in magmas, the models must be compared to the data on an anhydrous basis. Additionally, this leaves the initial magma H_2O content unconstrained. The H_2O of the mafic end of the Jindabyne trend (2–2.5 wt% given the scatter; Fig. 6h) provides a minimum estimate. Chappell & White (1992) suggested that for the LFB granites both S- and I-type magmas contained 3–4 wt% H_2O.

In the experiments of Naney (1983) at similarly low H_2O contents for a granodioritic system biotite appears only after plagioclase and orthopyroxene (for 200 MPa) and also after quartz (for 800 MPa). Hornblende only appears in experiments with greater than 4 wt% H_2O (and as the first phase only at $H_2O \geq 10$ wt%). Thus, neither biotite nor hornblende would be expected to be an important fractionating phase for models at the minimum water estimate. These phases might be more relevant for initial magma H_2O content above 4 wt%, but are still not expected to be the first or second phases to crystallise. Furthermore, Sisson & Grove (1993) demonstrated that hornblende stability is sensitive to Na_2O as well as to H_2O such that the hornblende stability observed for the 3.9 wt% Na_2O granodiorite of Naney (1983) is likely enhanced relative to the Jindabyne Suite, in which samples have only 2.2–3.1 wt% Na_2O (Fig. 6k).

The CO_2 contents measured for the Jindabyne samples are variable (0.03–0.16 wt%) and show no correlation with the SiO_2 or H_2O contents. The concentration (0.06 wt%) measured in the most mafic sample was taken as a baseline, and starting magmas vary from 0.05 to 0.08 wt% CO_2. Given the H_2O contents used and CO_2-H_2O, fluid-melt relationships shown in Behrens & Gaillard (2006), these would be near saturation at 200 MPa but undersaturated by a factor of 3–5 at 500 MPa.

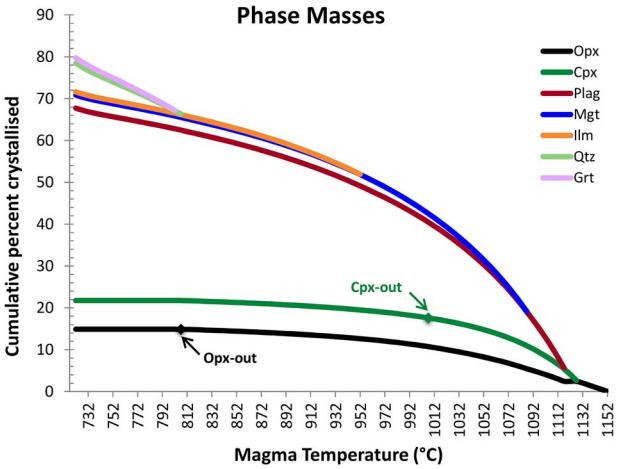

Fig. 8. Cumulative mass of phases fractionally crystallised from a mafic granitoid parental melt. The cumulative mass-magma temperature curves for each phase have been stacked to show their contribution to the overall cumulative percent of FC for model Jind03. The high temperature end of each curve indicates the first appearance of that phase, and the point at which a phase ceases crystallising is marked.

Liquid line of descent models

In this section, we present and discuss MCS FC models, including examples with the closest fit to the data. The detailed explanation of the process that led to the best-fit models is presented in the Supplementary Materials. Table 3 outlines the range of input parameters tested, while the full set of input parameters for these models are tabulated in the Supplementary Materials.

Baseline fractionation model

Firstly, it is instructive to examine the geochemical evolution and phase relations for FC of a magma represented by the most mafic sample of the Jindabyne Suite as a sort of 'baseline' model. Using sample KB139 (Grosses Plain pluton, Jindabyne Suite, $SiO_2 = 55.5$ wt%, $H_2O = 1.8$ wt%) as the parental magma, model Jind03 simulates the FC of this magma at 350 MPa until ~20 wt.% of the original liquid remains. Fig. 8 shows the cumulative masses of phases fractionated as functions of magma temperature, illustrating the paragenetic sequence: orthopyroxene (opx), clinopyroxene (cpx), plagioclase (plag), magnetite (mgt), ilmenite (ilm), quartz (qtz), and garnet (grt).

This sequence of changing liquidus phases manifests as 2–4 discernible segments in trends on Harker diagrams, depending on what major element oxides are considered (Fig. 9). The trends for K_2O and H_2O vs. SiO_2 show linear enrichment between the mafic starting composition and the qtz-in point, whereas MgO and Na_2O exhibit smooth curved variations over the same SiO_2 range. Small but distinct segments are seen among the most mafic compositions for Al_2O_3, Fe_2O_3, FeO and CaO before these oxides enter simple curved or linear trends for the majority of the magma evolution (up until qtz-in). These mafic segments contain subtle variations that end between 55.7 and 56.6 wt% SiO_2, depending on the element, corresponding to the appearance of plagioclase then magnetite on the liquidus. Thus, the interval between mgt-in at 56.6 wt% SiO_2 and qtz-in/opx-out at ~70 wt% SiO_2 produces very simple geochemical trends for almost all major element oxides. The magma evolution for TiO_2 involves different degrees of enrichment followed by depletion according to the appearance of magnetite then ilmenite. With the

Table 2: Amphibole grain average compositions and thermobarometry

Pluton	Round Flat	Round Flat	Round Flat	Jindabyne	Jindabyne	Jindabyne	Moonbah	Moonbah	Moonbah
Sample	KB05	KB05	KB05	KB20	KB20	KB18	KB25	KB25	KB25
Grain No.	15	16	17	18	19	20	21	22	23
n	4	1	6	1	1	8	2	2	4
SiO2	47.0	46.3	47.0	47.3	48.0	46.6	52.8	48.0	49.1
TiO2	1.09	1.11	0.80	0.69	0.43	0.38	0.28	0.48	0.59
Al2O3	8.0	8.2	7.7	7.1	6.6	7.1	1.7	6.7	8.1
V2O3	0.12		0.04	0.05					
Cr2O3				0.02					
Fe2O3									
FeO	15.1	15.5	15.7	16.2	16.3	18.0	21.4	15.7	13.3
MnO	0.53	0.51	0.64	0.63	0.69	0.83	2.23	0.73	0.61
MgO	13.3	12.7	12.9	12.5	12.8	11.4	16.4	13.0	13.2
CaO	11.1	11.3	11.1	11.1	11.2	11.2	2.5	10.6	10.6
K2O	0.39	0.36	0.32	0.64	0.56	0.55	0.13	0.29	0.36
Na2O	0.88	0.86	0.84	1.03	0.84	0.82	0.23	1.05	1.20
SO3	0.07		0.04		0.03				
Cl	0.13	0.12	0.11	0.15	0.12	0.03			0.06
Total	97.78	96.95	97.28	97.37	97.58	96.93	97.76	96.62	97.00
Site Allocation									
T site									
Si	6.76	6.75	6.81	6.91	6.99	6.88	7.74	6.97	7.07
Al	1.24	1.25	1.19	1.09	1.01	1.12	0.26	1.03	0.93
C site									
Al	0.13	0.16	0.13	0.14	0.11	0.11	0.03	0.12	0.44
Ti	0.12	0.12	0.09	0.08	0.05	0.04	0.03	0.05	0.06
V	0.01	0.00	0.01	0.01	0.00	0.00	0.00	0.00	0.00
Cr	0.00	0.00	0.00	0.00	0.00	0.00	0.00	0.00	0.00
Fe3+	1.12	0.99	1.15	0.91	0.96	1.05	0.21	1.14	0.69
Mg	2.86	2.77	2.79	2.72	2.78	2.51	3.57	2.82	2.82
Fe2+	0.70	0.89	0.76	1.07	1.02	1.17	1.15	0.77	0.91
Mn	0.06	0.06	0.08	0.08	0.09	0.10	0.00	0.09	0.07
B site									
Mg	0.00	0.00	0.00	0.00	0.00	0.00	0.00	0.00	0.00
Fe2+	0.00	0.00	0.00	0.00	0.00	0.00	1.26	0.00	0.00
Mn	0.00	0.00	0.00	0.00	0.00	0.00	0.28	0.00	0.00
Ca	1.71	1.77	1.72	1.73	1.75	1.76	0.40	1.66	1.64
Na	0.24	0.23	0.24	0.27	0.24	0.23	0.06	0.30	0.33
A site									
Na	0.00	0.01	0.00	0.02	0.00	0.00	0.00	0.00	0.00
K	0.07	0.07	0.06	0.12	0.10	0.10	0.02	0.05	0.07
Thermobarometry									
T (°C)	805	799	797	774	758	767		786	793
1 s.d.	16	22	20	22	22	9		4	33
P (kbar)	1.58	1.58	1.48	1.25	1.10	1.24		1.23	1.68
1 s.d.	0.09	0.19	0.15	0.15	0.13	0.09		0.08	0.30

exception of K_2O, no trends for major element oxides plotted against SiO_2 are exact matches for the geochemical variation observed in the Jindabyne Suite (Fig. 9). Particularly, relative to the data, the modelled trends markedly overestimate the degree of Fe_2O_3 and MgO depletion with increasing SiO_2, and the distinctly non-linear TiO_2-SiO_2 trend consistently overestimates the TiO_2 content at a given SiO_2 content.

The role of pressure

For the same starting composition at higher pressures, mostly the same minerals are involved and generally at similar stages. Increasing pressure delays the onset of plagioclase crystallisation and stabilises quartz and garnet at higher temperatures and lower SiO_2 contents. The main effect of the early transition from opx to grt crystallisation is to cause steepening of the FeO depletion (Fig. 9). Changes to pyroxene stability also affect MgO, Fe_2O_3, FeO and CaO during the most mafic segment of the compositional range. The suppression of plagioclase crystallisation at high pressure leads to greater enrichment in Al_2O_3 in that range, which shifts the main segment of the trend as shown in Fig. 9b.

At pressures of 150 to 250 MPa, the modelled FC trends differ only slightly from the 350 MPa simulation for most major elements (Fig. 9). There are further shifts in the appearance of phases (e.g. garnet does not crystallise), resulting in more consistent liquidus

Table 3: Summary of MCS model input parameters, including the range across all models

Parameter	Range	Jind18	Jind22	Jind28	JndA56	JndA59	JndA65
System pressure (bar)	1500–7000	3500	3500	4500	3500	3500	3500
Magma initial temperature (°C)[1]	1130–1500	1250	1250	1250	1250	1250	1250
Wallrock initial temperature (°C)	600–680[3]	-	-	-	680	680	680
Wallrock mass/magma mass (Λ)[2]	0.45–1.3	-	-	-	1.1	1.1	0.85
Wallrock critical melt fraction	0.05	-	-	-	0.05	0.05	0.05
Magma initial composition							
SiO_2	53.1–63.9	58.28	57.38	57.55	58.00	56.83	56.09
TiO_2	0.53–1.41	0.599	0.593	0.593	0.599	0.587	0.644
Al_2O_3	14.3–18.6	17.27	16.55	16.46	16.85	16.51	17.19
Fe_2O_3	1.68–2.90	2.276	2.238	1.893	2.650	2.596	2.034
FeO	3.20–6.57	4.144	4.071	3.768	4.430	4.341	4.233
MnO	0.090–0.190	0.0958	0.0957	0.0956	0.0958	0.0939	0.1147
MgO	2.41–5.14	4.692	3.922	3.108	4.900	4.801	3.805
CaO	4.77–8.82	6.354	6.170	6.569	6.598	6.465	6.983
Na_2O	1.80–4.16	2.446	2.378	2.391	2.500	2.450	2.306
K_2O	0.91–3.09	1.223	1.435	1.415	1.195	1.171	1.419
P_2O_5	0.094–0.521	0.0998	0.1081	0.1052	0.998	0.0978	0.1119
H_2O	0.80–8.00	2.456	5.000	6.000	2.022	4.000	5.000
CO_2	0.030–0.230	0.0579	0.0574	0.0574	0.0579	0.0567	0.0744
Wallrock initial composition[4]							
SiO_2	62.6–89.8	-	-	-	64.97	64.97	66.29
TiO_2	0.20–0.76	-	-	-	0.586	0.586	0.598
Al_2O_3	4.3–15.9	-	-	-	15.69	15.69	14.77
Fe_2O_3	0.13–1.17	-	-	-	0.363	0.363	0.371
FeO	0.58–5.05	-	-	-	4.904	4.904	5.015
MnO	0.030–0.101	-	-	-	0.0490	0.0490	0.1001
MgO	0.74–3.22	-	-	-	1.962	1.962	2.004
CaO	0.22–3.50	-	-	-	3.160	3.160	2.258
Na_2O	0.12–5.56	-	-	-	4.904	4.904	4.492
K_2O	0.14–4.53	-	-	-	0.617	0.617	0.993
P_2O_5	0.098–0.340	-	-	-	0.0981	0.0981	0.1101
H_2O	0.40–3.50	-	-	-	2.694	2.694	3.000
CO_2	0–0.66	-	-	-	0	0	0

[1]This is the temperature at which the 'find liquidus' operation starts. The magma chamber simulation starts at the relevant liquidus.
[2]Resident magma initial mass is 100 units.
[3]740°C for stoped blocks of WR.
[4]The compositions used are shown in Fig. 11 relative to a compilation of sedimentary rock compositions, detailed in the Supplementary Material.

assemblages for most of the composition range, producing generally smoother trends. There is a distinct effect of pressure on the ASI-SiO_2 trend; however, because ASI (the aluminium saturation index: $ASI = Al_2O_3/(CaO + Na_2O + K_2O)$, using mole per 100 g) is sensitive to multiple subtle shifts in the geochemical evolution of models, this effect will *not* be relevant to all starting compositions.

Magma initial composition variations and best-fit models

A range of initial compositions for the magma were tested to find potential FC models for the Jindabyne Suite. Some of the most well-fitting models that result from a series of exploratory models are discussed below.

Models run using diverse mafic samples as starting compositions allow a greater variety of possible geochemical trends to be explored. It also allows the identification of certain general features in such trends that are common and persistent for FC models in the broadly granitic compositional space of interest here. Understanding this broader range of LLDs is valuable for consideration of *in situ* crystallisation models, in which the magma evolution relies on a series of different LLDs.

Shifting the starting composition to higher SiO_2 contents (such that parts of the linear trends would be explained as liquids and the more mafic parts as cumulate compositions) shortens some parts of the trends, but the overall shapes of the trends change very little. Ultimately, the ways in which the FC trends deviate from the data are not affected by reasonable shifts in the starting compositions along the linear regressions, although the degree of deviation can be dampened somewhat.

More diverse changes in starting composition (higher FeO, MgO, and K_2O at a given SiO_2, higher FeO at a given MgO, higher Fe_2O_3 at a given TiO_2, and lower Al_2O_3 and Fe_2O_3 at a given SiO_2) were also tested, since there is some scatter in the Jindabyne data (Fig. 6). Such tests showed that some features of FC models that are relatively robust. Barring large changes in starting composition outside the Jindabyne data, the basic shapes of the MgO vs. SiO_2 and K_2O vs. SiO_2 evolutions are very consistent from model to model. Additionally, enrichment of H_2O is a persistent feature, consistent with the fractionation of anhydrous phases (exsolution of pure water only occurs in advanced stages). The variations in TiO_2 contents are the most sensitive to changes in the starting composition.

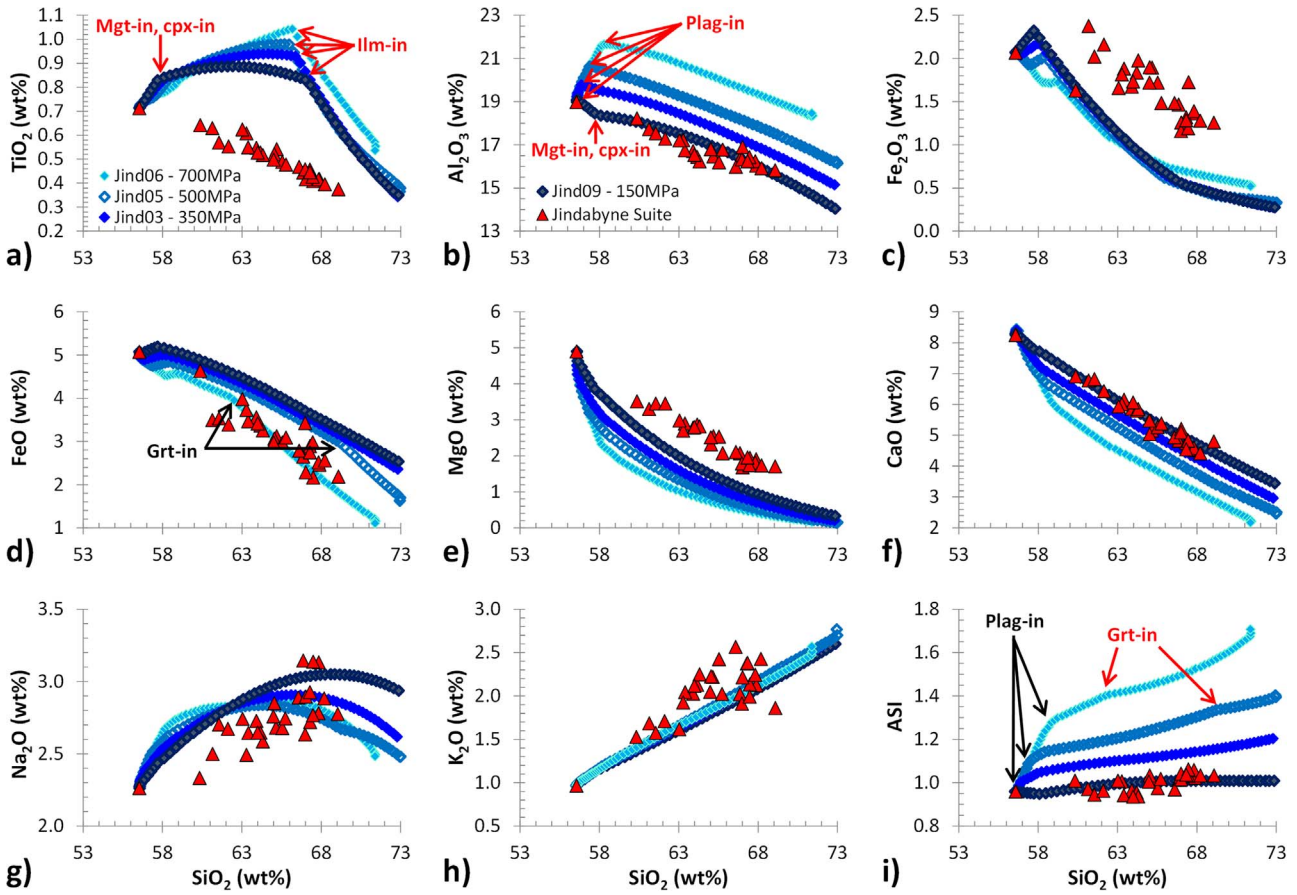

Fig. 9. Harker diagrams comparing the output of simulations at various pressures with the compositions of the Jindabyne Suite granite samples. The simulations have the same initial composition (55.5 wt% SiO_2, 1.8 wt % H_2O). Note the linear or simple curves that occur for many oxides and the general increase in the deviation of the models from the data with increasing model pressure – the model is typically closest to the data for 150–350 MPa. The trends have been trimmed to just after the point at which quartz enters the liquidus assemblage (~70 wt% SiO_2).

Four candidate best-fit models (Jind14 & Jind16–18; see Supplementary Material for details) were produced, and they all have many aspects in common. The Harker diagrams for models Jind16 and Jind18 are shown in Fig. 10. These models start at compositions slightly less mafic than for Jind03 (57.6–59.2 compared to ~55.5 wt% SiO_2). Once ilmenite starts precipitating the trends for these models are similar to those for the previous models for all major elements. Despite decent fits in terms of FeO, CaO, and K_2O, the issues with TiO_2 and Fe_2O_3 persist.

As illustrated in Fig. 10, increasing the magma's initial water content mostly affects TiO_2, Fe_2O_3 and Na_2O. Particularly, this results in a shift of the TiO_2-SiO_2 trend from enrichment to depletion relative to the Jindabyne Suite, coupled to increased depletion of Fe_2O_3 at the beginning of the liquid evolution. With increasing magma initial H_2O the models show slightly enhanced enrichment of Na_2O. There are more subtle changes to the trends in Al_2O_3-CaO-K_2O-SiO_2 space, resulting in a general shift towards greater lowering of ASI with increasing SiO_2 contents. Thus, although it is possible to achieve an improvement upon the trends of Jind16 and Jind18 with respect to TiO_2 and Na_2O by selecting the appropriate starting composition with 5% H_2O (Jind22), the cost is that the model greatly underestimates the Fe_2O_3 content for the majority of the SiO_2 range, and achieves no improvement with respect to ASI.

Finally, we note that enrichment of H_2O in the magma still occurs for models with the highest initial water contents (6–8 wt%), although they eventually show decreases in water content once the fluid fractionated is pure H_2O and, later, when biotite fractionates. The relatively high water contents of the modelled magma compositions can be reconciled with the lower water contents of the samples if additional fluid is exsolved from the magmas and escapes when the magmas ascend to emplacement level.

Assimilation-fractional crystallisation

The modelling thus far indicates that FC of I-type granite compositions at various pressures is consistently expected to produce LLDs that either markedly deviate from linearity or exhibit linear trends of drastically inappropriate slopes for certain major element oxide bivariate plots. A series of MCS models were run to test whether assimilation of WR melt during FC could overcome these problems and produce LLDs matching the linear geochemical trends observed in the Jindabyne Suite. Modelling started with the low water magma initial composition of Jind18 and tested higher water contents after other aspects of the parameter space had been explored.

The compositions of sedimentary and metasedimentary rocks from southeastern Australia (including the Ordovician to Silurian LFB sedimentary rocks), New Zealand and Antarctica were compiled

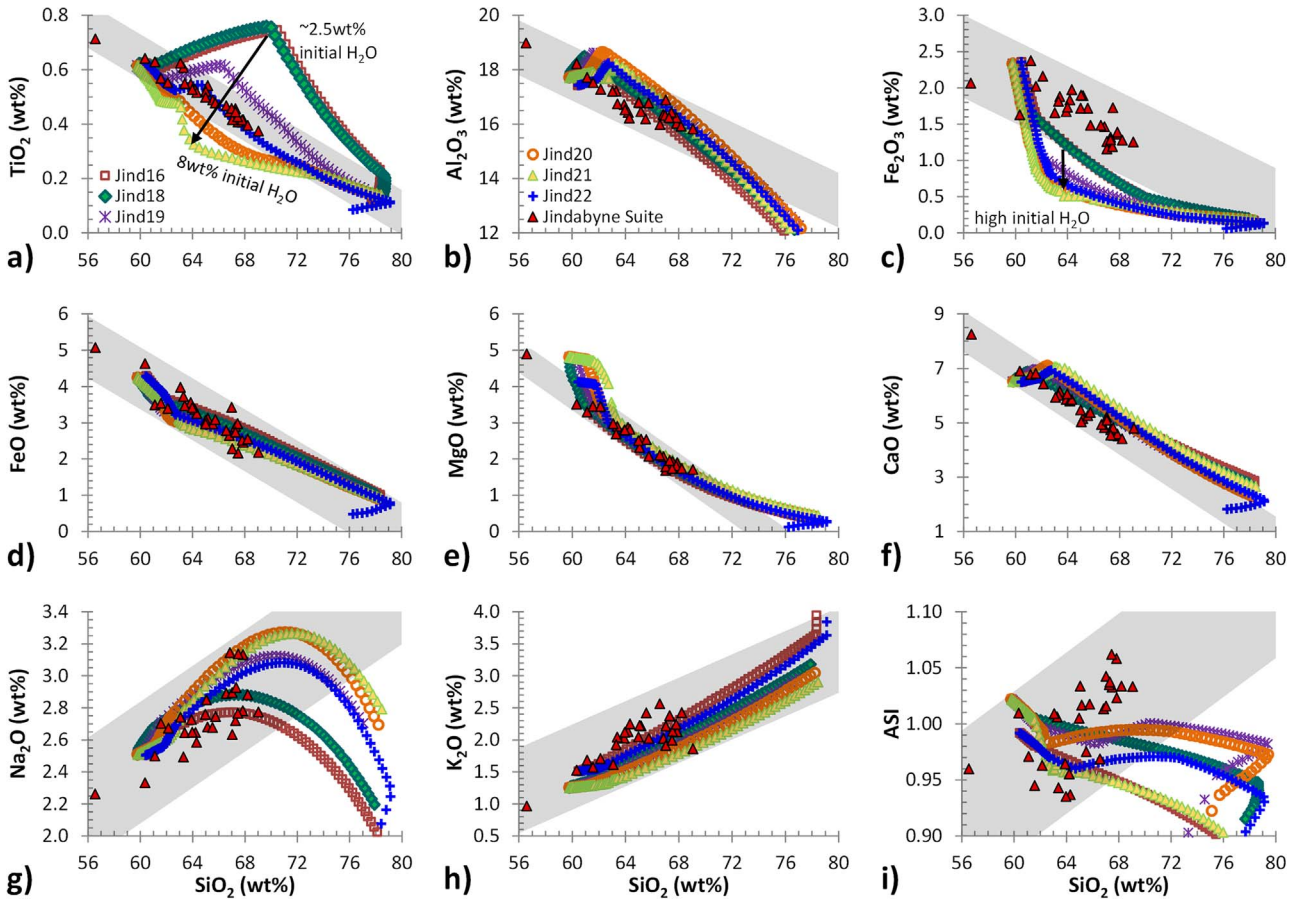

Fig. 10. Comparison between the geochemical trends of best fit models for low water contents (Jind16 & Jind18) and those produced by increasing starting magma water content. Shaded in grey is the Jindabyne line of best fit expanded to a band encompassing the data. Note that a generally better fit than those in Fig. 9 is found for a shift in starting composition to slightly higher SiO_2. Among the low water models there is a general concordance between the models and the Jindabyne Suite for most oxides except TiO_2 and Fe_2O_3. a) and c) illustrate that increasing water content causes a shift (indicated with an arrow) towards depletion in TiO_2 and Fe_2O_3 relative to SiO_2. It is clear in i) that all of these models fail to match the ASI evolution of the Jindabyne Suite.

to characterise the geochemical diversity of possible supracrustal assimilants (Table 3; Fig. 11; see Supplementary Materials for a detailed list). Since the most obvious deviations of the FC model trends from the data are associated with compositional changes early in the fractionation of the magma, if assimilation is to improve the fit, WR melt needs to be introduced into the magma relatively early; therefore, a reasonably high 'pre-warmed' WR initial temperature (600–680°C) is utilised to ensure minimal magma evolution before the WR melts and reaches the melt percolation threshold (critical melt fraction of 0.05, FmZero in MCS jargon).

The best-fit assimilation–fractional crystallisation models

From comparison of the geochemical trends for the AFC models with those for Jind18 (Fig. 12) it can be observed that the assimilation of WR melt distinctly alters the compositional changes in the magma that fractionation causes. For example, among the many models tested it is typical for assimilation to dampen the TiO_2-enrichment of the magma to varying degrees, at least initially, because early WR melt is generally Ti-poor. Since the WR continues to melt as fractionation progresses, the WR melt composition also evolves so that eventually assimilation will contribute relatively Ti-rich melt to the magma, leading to late TiO_2-enrichment of the magma. Since the extent of these two related effects is strongly dependent on the WR composition, mass and initial temperature (as well as the effect of magma water content on Ti), a number of models were run attempting get the best balance of these effects to produce a LLD matching the Jindabyne TiO_2-SiO_2 trend.

The extent to which magma trends in AFC models differ from each other and from FC-only models for any particular bivariate element plot depends partially on how the concentrations of elements in WR melt compare to the concentrations in the magma and the tendency of FC to enrich or deplete that element. The magma evolution in Fe_2O_3-FeO-MgO-SiO_2 space is relatively insensitive to the tested variations in WR composition. Since the WR melts consistently have lower concentrations of the Fe-Mg oxides than the magma, assimilation acts to decrease their concentration in the magma; however, fractionation of mafic minerals is more significant for the depletion of the magma in these oxides (Figs 9 and 10). In contrast, fractionation enriches the magma in K_2O and SiO_2, which are also typically more abundant in the assimilated WR melt than in the magma.

Certain changes in WR composition will alter the effect of assimilation on the magma LLD because such differences correspond to different WR mineral assemblages. While some changes simply change the proportions of WR phases (e.g. the proportion of quartz and micas in different LFB sediments), others significantly alter the

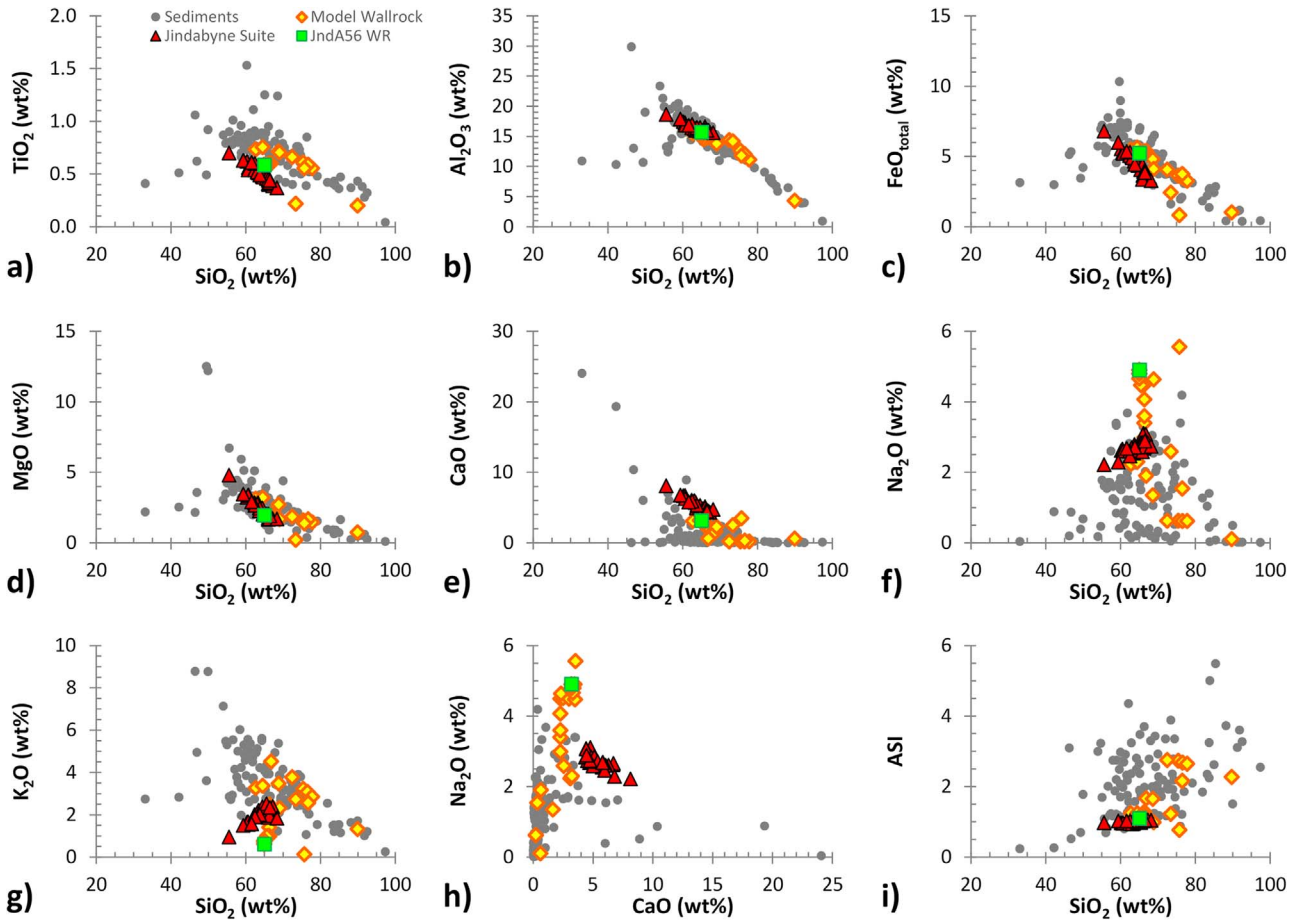

Fig. 11. Comparison of the compilation of (meta)sedimentary rocks with the Jindabyne Suite. The compositions used as WR are shown and the WR used in JndA56 (one of the best fitting AFC models) is separately highlighted. Sedimentary compositions from: Bowes. (1954); Milnes (1973); Nathan (1976); Turner *et al.* (1993) and Wyborn & Chappell (1983).

melting regime because different minerals are stable at the solidus. For example, the differences between WR partial melting in which muscovite dehydration is accompanied by K-feldspar melting vs. muscovite dehydration producing peritectic K-feldspar vs. muscovite being absent at the solidus of the WR are important for magma trends in CaO-Na_2O-K_2O-SiO_2 space.

Following the exploration of the effects of various changes to input parameters upon magma LLDs, iterative fine tuning of the AFC model was achieved through changes to WR composition, initial temperature and mass, model pressure and magma initial composition (detailed in the Supplementary Materials). This process yielded a few models (JndA42, JndA55 & JndA56; shown in Fig. 12) that fit the Jindabyne Suite reasonably well, and all involve relatively low initial magma water contents (~2 wt%; based on measured water in samples as is Jind18).

Without consideration of the relationship between peraluminosity and SiO_2 contents, the best fit to the data is found for simulation JndA42 (Fig. 12). Even so, the best-fit models slightly underestimate the Fe_2O_3 concentrations for most of the compositional range and overestimate TiO_2 for the high-SiO_2 samples. Simulations JndA55 and JndA56 match the data in almost all of the same ways as JndA42 except that the overall increase in magma ASI with increasing SiO_2 contents (broadly matching the data) achieved by JndA55–56 comes at the cost of: (1) Na_2O vs. SiO_2 and CaO trends that are shallower than an ideal fit to Jindabyne Suite, and (2) K_2O-SiO_2 trends that are slightly shallower than that of JndA42.

Models JndA59, JndA60 and JndA61 used 4, 5 and 6 wt% H_2O, respectively, for the magma initial composition, with the other oxides kept in the same proportions as for JndA56 (~2 wt% H_2O). Of these the closest match for the Jindabyne Suite trends is JndA59. Simulation JndA59 reproduces the Jindabyne data slightly better than does JndA56 in some respects and slightly worse in others (Fig. 12). As was observed for FC-only simulations with increased H_2O, the degree of Fe_2O_3 depletion is greater in JndA59 (and JndA60–61) than JndA56. Since the JndA56 Fe_2O_3-SiO_2 trend is one of the closest matches to the Jindabyne trend (i.e. it least strongly underestimates the Fe_2O_3 content for a given SiO_2 concentration) out of models JndA01–56 (although some, like JndA55, are very similar), any other model used as the basis for elevated water content simulations (e.g. testing JndA42 modified to have 4 wt% H_2O in the magma) would perform as poorly or worse than JndA59 in this particular regard. Thus, the models Jnd55–6 and JndA59 represent the most well-fitting AFC LLDs for the Jindabyne Suite.

Therefore, a thermodynamically constrained AFC model that produces liquid magma evolutions matching the Jindabyne Suite major element geochemistry in many aspects *can* be produced, although the model is unable to be reconciled with some details of the data. Additional sensitivity tests involving bulk assimilation of stoped WR

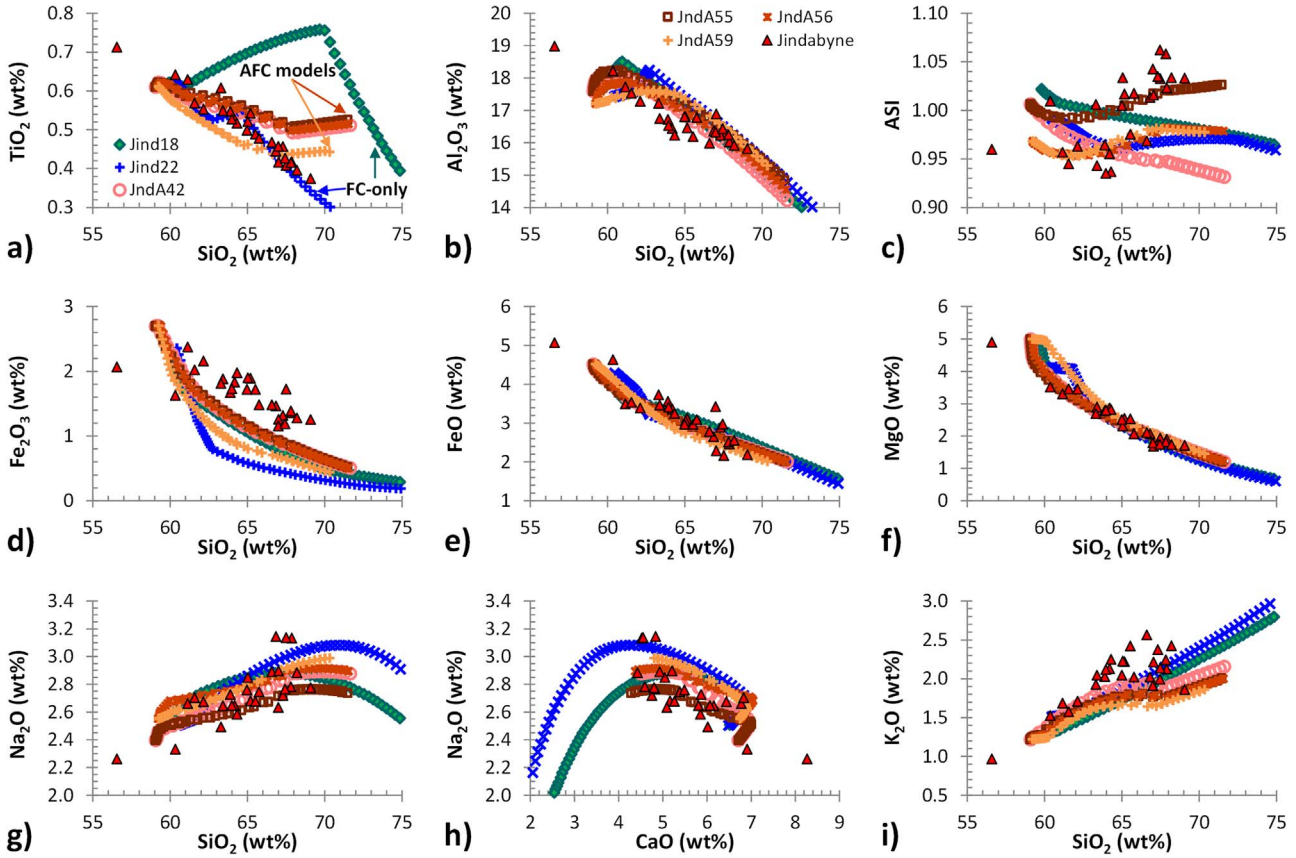

Fig. 12. Comparison between the geochemical trends produced by FC and those produced with AFC. In a) the AFC models JndA42, JndA55 and JndA56 differ markedly from Jind18, and increasing the water content of JndA56 to 4% for JndA59 also creates a noticeable shift in the trend. c) Note that models JndA55, JndA56 and JndA59 show an overall increase in ASI, unlike the best fit FC-only models and earlier AFC models (e.g. JndA42). The offset between JndA55 and JndA56 for this plot is related to a shift in magma starting composition CaO-Na_2O-SiO_2 space. In d) although the low water content models (Jind18, JndA42, JndA55 & JndA56) are nearly indistinguishable, the effect of higher water content on Fe_2O_3 can be seen for both the AFC model (JndA59, 4% water) and the FC-only model (Jind22, 5% water). On most other plots the AFC and FC models are very similar, although the FC models extend to higher SiO_2, which is accompanied by depletion in Na_2O.

blocks did not improve the fits (Supplementary Materials). The trace element evolutions of the best fitting models are examined below to further assess their applicability.

Trace element modelling

Two of the presented best-fit models, Jind18 for FC and JndA56 for AFC, were chosen for trace element modelling. Although described as 'best-fit' models, both Jind18 and Jind22 FC-only models have prominent deviations from the Jindabyne major element data. Nevertheless, Jind18 serves as a comparison for AFC model JndA56.

The trace element modelling inputs and outputs are included in the Supplementary Material (this encompasses all of the basic MCS output, including major element contents and phase masses). Trace elements Ba, Rb, Sr, Pb, Th, Nb, Sc, La, Ce, and Nd were chosen for the modelling based on data availability and because the data show clear correlations with regards to these elements. The starting magma composition was set based upon regression of the Jindabyne trace element data to the SiO_2 content of the magma. Since the WR major element composition is not that of a specific sedimentary rock sample, reasonable trace element concentrations were linked to the major element concentrations based on correlations between the selected trace elements and the TiO_2, Al_2O_3, FeO, CaO, Na_2O and K_2O contents for the LFB sedimentary rocks. The Sr isotope composition of the starting magma and the WR were set to those of sample KB22 of the Jindabyne Tonalite and the average of LFB sediment samples, respectively (McCulloch & Chappell, 1982; McCulloch & Woodhead, 1993; Iles, 2017). Mineral-melt partition coefficients were set based on published data, where possible leveraging the P–T-composition information of the MCS model to constrain the values. The ranges of partition coefficients input for each phase for the selected elements are shown in Table 4, along with the literature sources. Mineral-fluid partition coefficients for the WR were set to 1; a sensitivity study showed that the magma compositional evolution is effectively independent of mineral-fluid trace element partitioning for this model.

The geochemical trends for Jind18 and JndA56 are shown with the Jindabyne Suite data in Fig. 13. Three trace elements (Sr, Nb and Pb) display nearly identical behaviour in both models and Sr and Nb match the data fairly well. A good match between the data and Jind18 can be observed for some trace elements, but there is notable divergence of the FC model from the data for the Sc-SiO_2 plot. In contrast, for the AFC model JndA56, several trace elements show much more marked enrichment in the model than is observed in the Jindabyne Suite. The trace elements modelled (except Sr and Sc) behave incompatibly during fractionation of the magma. The common cause of divergence between the FC and AFC models is

Table 4: Summary of partition coefficients used in models. A range is given where composition and temperature dependent values were used

Phase	Rb	Sr	Nb	Ba	La	Ce	Nd	Pb	Th	Sc
Amphibole[1]	0.18	6.4	1.4	0.21	0.71	1.3	3.4	0.37	0.25	7.39
Biotite[2]	6.98	0.01	24.5	0.58	0.015	0.0298	0.059	0.04	0.01	42.4
					0.016	0.032	0.062			
Clinopyroxene[3]	0.0035	0.08	0.021	0.0019	0.094	0.191	0.515	0.13	0.007	7.39
					0.102	0.199	0.652			
Garnet[4]	0.115	0.126	2.62	0.112	0.014	0.064	0.797	0.044	0.0026	1.19
					0.369	1.164	7.31		0.34	1.60
Ilmenite[5]	0.01	0.04	1.9	0.01	$1.5*10^{-7}$	$2.5*10^{-6}$	$5.4*10^{-5}$	0.01	0.01	4.6
			66.5		$1.3*10^{-6}$	$1.4*10^{-5}$	$1.9*10^{-4}$			15.4
Leucite[6]	4.75	0.0015	0.04	0.18	0.0011	0.0035	0.0035	0.0073	0.0035	0.072
Magnetite[7]	0.01	0.14	0.46	0.1	0.106	0.205	0.366	0.71	0.0032	2.7
			15.8		0.177	0.279	0.415		0.0213	66.8
Orthopyroxene[8]	0.0002	0.0044	0.015	0.0058	0.0039	0.0065	0.016	0.048	0.01	1.2
	0.8697	0.0346		0.3627	0.063	0.089	0.165	27.7	1.39	45.3
Plagioclase[9]	0.01	2.57	0.0016	0.21	0.121	0.112	0.088	0.45	0.028	0.014
	0.089	8.94	0.3333	1.22	0.329	0.314	0.266	0.765	0.131	0.27

[1]Constrained from: Brophy *et al.* (2011), Dalpé and Baker (2000), Marks *et al.* (2004) and Nehring *et al.* (2010)
[2]Constrained from: Bea *et al.* (1994) and Nash and Crecraft (1985)
[3]Constrained from: Hill *et al.* (2011), Kleine *et al.* (2000) and Klemme *et al.* (2002)
[4]Constrained from: Adam and Green (2006), Dwarzski *et al.* (2006), Kleine *et al.* (2000), Klemme *et al.* (2002), Koepke *et al.* (2003), McKenzie and O'Nions (1991), Philpotts and Schnetzler (1970), Rubatto and Hermann (2007), Shimizu (1980), Sweeney *et al.* (1992) and Tuff and Gibson (2007)
[5]Constrained from: Acosta-Vigil *et al.* (2012), Klemme *et al.* (2006), Nash and Crecraft (1985) and van Kan Parker *et al.* (2011)
[6]Constrained from: Fabbrizio *et al.* (2008), Minissale *et al.* (2019) and Wood and Trigila (2001)
[7]Constrained from: Bacon and Druitt (1988), Ewart and Griffin (1994), Luhr and Carmichael (1980), Nash and Crecraft (1985) and Nielson *et al.* (1992)
[8]Constrained from: Bédard (2007)
[9]Constrained from: Bédard (2006) and Ren *et al.* (2003)

that these elements are mostly also incompatible during melting of the WR, which leads to their enrichment in the WR melt that is assimilated in the early stages of the AFC process, creating much stronger enrichment of the elements in the magma than FC alone would cause. For the LREE and Th, the over-enrichment of the magma (Fig. 13f, g and i) is potentially due to monazite not being handled by MELTS in the WR. In the models the steep increase in LREE and Th in the magma is caused by their high concentrations in the earliest WR melt assimilated by the magma; however, these elements are likely controlled by monazite, which would buffer the WR melt to lower concentrations. While the 1st-assimilated melt in JndA56, for example, has 208 ppm La and 382 ppm Ce (compared to magma with 16 and 36 ppm, respectively), assuming LREE are controlled by monazite solubility would instead give *68 ppm total LREE* for the same first WR melt, according to the calibration of (Rapp *et al.*, 1987). Thus, were monazite solubility integrated in to the MCS models, the AFC trends would likely show a different trends for magma LREE and Th. This does not ameliorate the enrichment of Rb (Fig. 13c). Although there is some uncertainty in the partition coefficients, no reasonable change in the partitioning behaviour of Rb would be sufficient to prevent this enrichment.

A clear contrast between the models is that between signatures of open- vs. closed-system behaviour. The La/Nb ratios of the samples are scattered but essentially uncorrelated with SiO_2 contents, which is also the case for Jind18 until, at ~67 wt% SiO_2, ilmenite starts crystallising and the proportion of magnetite in the liquidus assemblage decreases (Fig. 13). In contrast, as soon as assimilation begins in JndA56, the La/Nb ratio of the magma dramatically increases until, at ~64% SiO_2, the magma and WR melt have similar La/Nb ratios; however, accounting for role of monazite in the WR would likely alter this trend. The increase in the Sr isotope ratio of the magma in the AFC models is quite minor, because of residual Sr-retaining plagioclase in the WR. Given that the existence of any correlation between the $^{87}Sr/^{86}Sr_i$ values and SiO_2 contents of the granite bulk-rock samples is equivocal, either the FC (with no change in $^{87}Sr/^{86}Sr_i$) or AFC models could be compatible with the data. This highlights an important observation from the modelling: AFC will not necessarily produce Sr isotope variations large enough to be observed given analytical uncertainty.

Partial segregation models

All of the models run attempting to reproduce the Jindabyne Suite trends as LLDs of FC (±assimilation) were assessed using the criteria outlined in the Modelling Methods section for application to (A)FC-SPS, (A)FC-CPS and FC-driven *in situ* crystallisation models. One consideration for the AFC models is that invariably they simply do not extend to SiO_2 contents as high as FC-only models. Because MCS is an energy-constrained modelling tool, the extent of an AFC run is based on the thermal equilibration of the magma with WR as the former cools and crystallises and the later heats up and melts – that is, the simulation stops if when the magma and WR reach the same temperature even though there may still be substantial liquid in the magma. One can imagine the coupled magma-WR system slowly cooling together after thermal equilibration, and thus take the crystallisation model further by simply running a FC-only simulation of the final magma composition of an AFC simulation. This consideration is taken into account when assessing the models

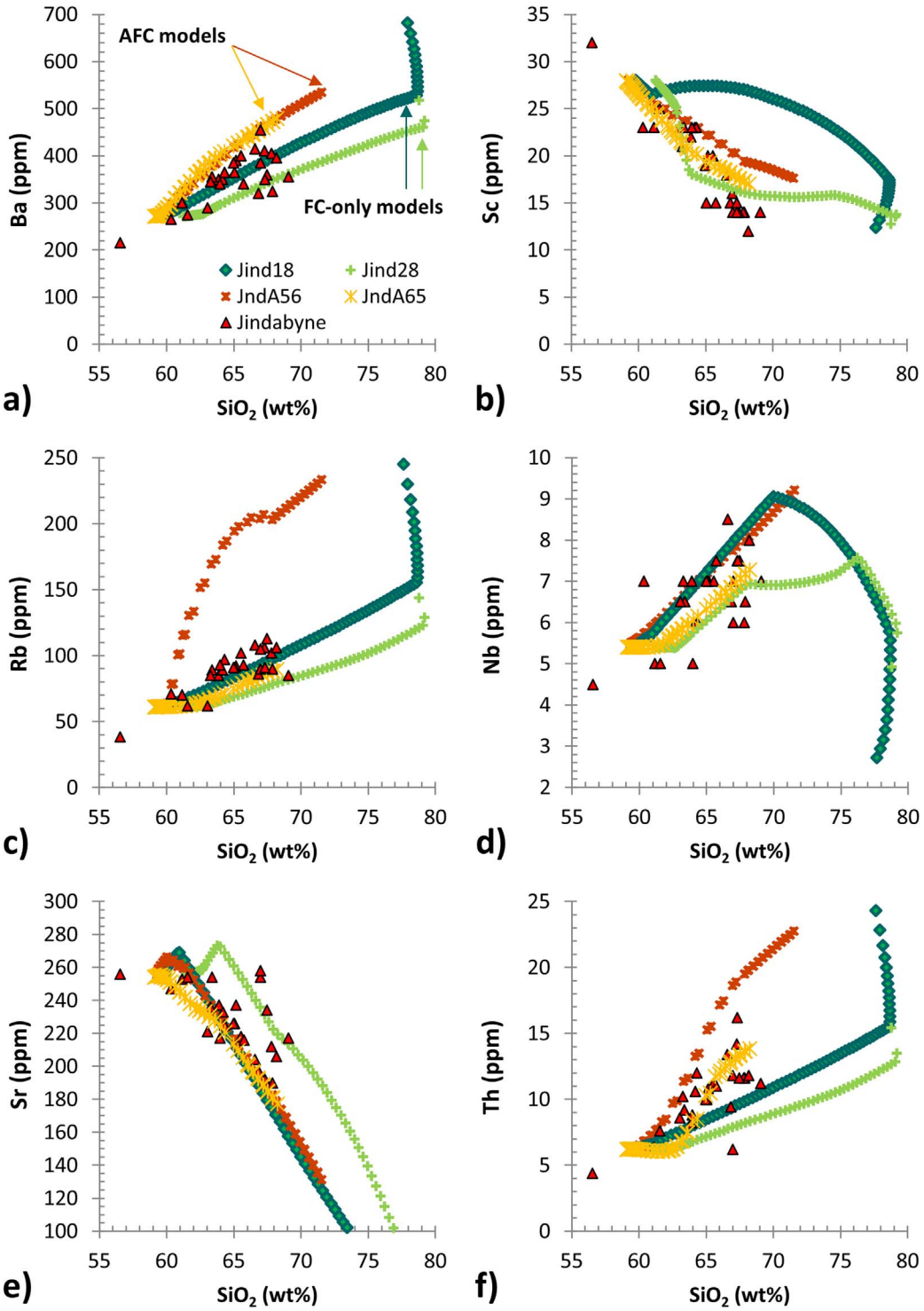

Fig. 13. Trace element and isotope trends for the FC-only (Jind18, Jind28) and AFC (JndA56, JndA65) models that best fit the major element data of the Jindabyne Suite, either as LLDs or used for partial segregation and *in situ* crystallisation modelling. Note the similarity between models for Nb, Sr and Pb, the mismatch between Jind18 and the data for Sc, and the mismatch between JndA56 and the data for Ba, Rb, Th, LREE and La/Nb. The use of a different WR compositions for JndA56 and JndA65 results in multiple differences in trace element enrichment in the magma, particularly for Rb and Th.

against the criteria for partial segregation and *in situ* crystallisation models.

Following the assessment of simulations Jind03–22 and JndA01–61 against the criteria, a set of additional simulations were run to provide more appropriate LLDs. Models Jind23–31 were based on Jind20 and Jind22 but with different pressures (250–450 MPa) and some changes to the input magma composition. New AFC simulations (JndA62–67) tested higher initial magma water contents

in JndA22 and JndA27, extending select AFC simulations with late-stage FC, adjusting starting magma particularly with respect to the oxides relevant to ASI, and increasing the mass of WR involved. Below we highlight some general issues with the expanded set of simulations for (A)FC-SPS/CPS models and illustrate which examples perform best.

Crystallisation with subsequent partial segregation

It is generally the case that, although the linear trends of the Jindabyne Suite data do extend to points on the modelled LLDs at both mafic and felsic ends for some Harker diagrams, they do not do so for all (or do not do so at a consistent stage of the magma evolution); therefore, all of the original FC-only models (Jind03–22) fail the criteria for subsequent partial segregation. As shown in Fig. 10, while the LLDs all cross the band of the Jindabyne regression in TiO_2-Fe_2O_3-SiO_2 space at very high SiO_2 contents, by that stage the other parameters (notably Na_2O and ASI) are too far from the Jindabyne trend for an FC-SPS model to be applicable. Similar issues for FC-SPS models can also be observed for the models in Fig. 9.

For AFC-SPS, the crystal-bearing magma that would undergo crystal-liquid sorting to generate a linear trend would be the mixture of the starting magma and all of the batches of assimilated melt. These magmas must (and typically do) have compositions still within the Jindabyne Suite data for the various simulations for the AFC-SPS model to work; however, the models will be inappropriate if the felsic ends of the LLD (the felsic melt component of those magmas) do not intersect the Jindabyne trend.

As for the FC-only models, the LLDs for JndA01-JndA61 do not have the requisite shapes across the major element space for AFC-SPS to reproduce the linear trends of the Jindabyne Suite. Particularly, the underestimation of Fe_2O_3 even once models were produced that corrected issues with TiO_2 enrichment, hinder AFC-SPS models. Although additional simulations (JndA62–67) lead to LLDs that overlapping the Jindabyne Suite data for many plots including ASI vs. SiO_2 and reach compositions along the extension of the Jindabyne Fe_2O_3-SiO_2 trend, assimilation shifts the crystal-bearing magma composition to such high SiO_2 contents that the segregation trend would only account for the most felsic samples. The mafic-intermediate portion of the Jindabyne trend could be explained by the evolution of the parental melt towards this crystal-bearing magma as assimilation proceeds; however, this two-part evolution creates curved and kinked sections in the overall trend, which are what the subsequent partial segregation idea was supposed to avoid and suggests these LLDs would be more fruitful as a basis for AFC with *concurrent* partial segregation.

One simulation that, from visual inspection of the LLD in comparison to the Jindabyne data, *does* meet the criteria for FC-SPS is Jind28. As such, a trace element model was generated for this simulation to check that the criteria are met also for trace elements. Visual inspection of the trends in Fig. 13 shows that this is the case, except for the underestimation of Pb enrichment. Fig. 14 illustrates three different FC-SPS trends based on Jind28. The trend lines extend from different points on the LLD to the parental magma composition, representing varying degrees of segregation crystals from a magma whose melt has evolved to that point on the LLD. Extension to compositions more mafic than the parental magma represent melt-depleted/cumulate-rich magmas (mushes or cumulate piles). In some plots the FC-SPS lines for 20, 34 and 44% crystallisation are approximately colinear and equally consistent with the Jindabyne data, but differences are evident in TiO_2-Fe_2O_3-MgO-Al_2O_3-Na_2O-ASI-SiO_2 space. As shown in Fig. 14, segregation after less crystallisation provides the best fit to the Jindabyne TiO_2-SiO_2 and ASI-SiO_2 trends, but more crystallisation provides a better fit in Fe_2O_3-SiO_2 space. Balancing these, the line based on segregation after 34% crystallisation (FC-SPS 3) provides a reasonable fit in all plots.

Crystallisation with concurrent partial segregation

The criteria for an LLD to be the basis of an (A)FC-CPS model are essentially less strict versions of the criteria for (A)FC-SPS; therefore, many of the original set of FC-only (Jind03–22) and AFC models (JndA01–61) fail to meet the criteria for CPS for the same reasons as for SPS. Given those criteria, Jind28 was deemed a suitable candidate for modelling FC-CPS (just as it was shown to be for FC-SPS). It exhibits similar trends to best-fit FC model (Jind22) on most plots but has the general increase in ASI with increasing SiO_2 contents required to meet the criteria for a FC-CPS model. The best candidates of all AFC simulations for producing a CPS model for Jindabyne are simulations JndA65–67. Simulation JndA65 was chosen for modelling trace elements. As shown in Fig. 13, the only departures of the trace elements from the criteria for AFC-CPS occurs for REE, which might reflect the lack of modelling of accessories. Otherwise, the trace element trends confirm that JndA65–67 are suitable for AFC-CPS.

In order to build a concurrent partial segregation model from an MCS model, the model output was first used to calculate the compositions of the instantaneous cumulate assemblage (the aggregate of all newly formed crystals at a particular step in the simulation). With this information we defined the composition of a crystal-bearing magma as the mixture of melt from a particular step and the crystal cargo present at that step. The crystal cargo at any step is made of the instantaneous cumulate for that step and some portion of the crystal cargo of the previous step. The fraction of the crystal cargo retained from one step to the next was set in consistent manner for all steps. Two approaches were tested. The first approach set a constant fraction of crystal cargo to be retained. In the second, a threshold crystallinity was set. Below this threshold the fraction retained from step to step is 1, and above it the fraction retained is set to hold the magma at the threshold. These two methods produce broadly similar (A)FC-CPS trends, although the former approach is more sensitive to the shape of the LLD.

Using the Jind28 simulation as the basis for FC-CPS models yields a close correspondence to the Jindabyne Suite trends for most Harker diagrams except Fe_2O_3-SiO_2 and ASI-SiO_2 (Fig. 15). Using either of the approaches to segregating crystals results in better matches to ASI-SiO_2 when crystal segregation is stronger (FC-CPS models approach the LLD), but these models exhibit strong depletion in Fe_2O_3 (as does the LLD; Fig. 15c). In contrast, greater retention of crystals in the magmas (particularly using crystallinity thresholds of 30–35%) produces FC-CPS models consistent with the Jindabyne Fe_2O_3-SiO_2 trend but restricts the modelled ASI to values lower than half of the samples (Fig. 15i).

For AFC-CPS, two models produce similarly good matches to the Jindabyne trends. The simulations JndA65 and JndA67 are identical in model input except for the mass of WR involved ($\Lambda = 0.85$ and 1.3, respectively). For both of these LLDs, the AFC-CPS trends resulting from either segregation approach become more restricted in SiO_2 range with increasing degrees of crystal retention. However, because lowering crystal retention draws the trends toward the LLDs, which exhibit strong early depletion in Fe_2O_3, the closest fits to the data involve compromise between the shape and position of the Fe_2O_3-SiO_2 trend and the SiO_2 range. Using JndA67 as the basis for the model, crystallinity thresholds of 19–22% allow AFC-CPS to

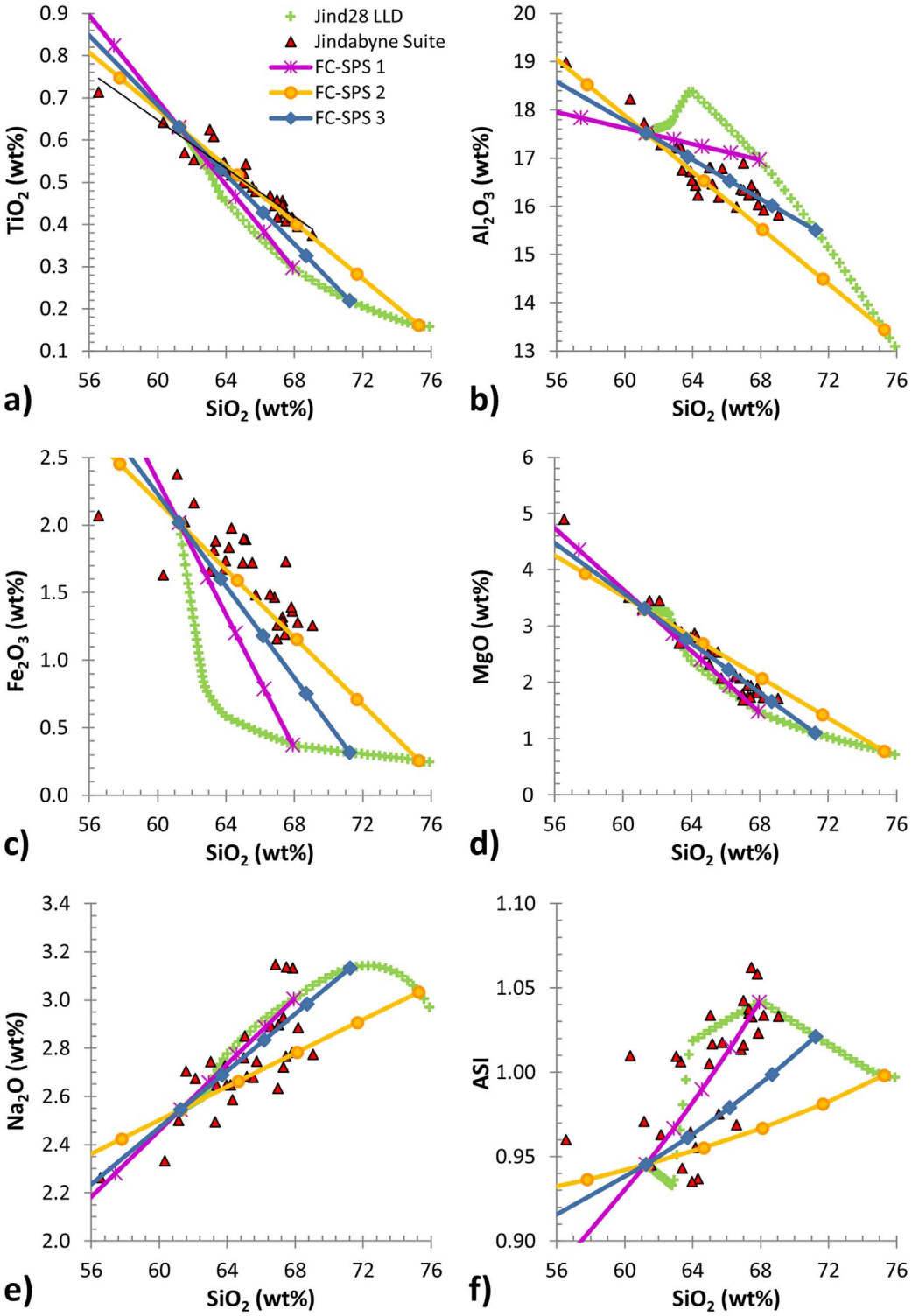

Fig. 14. FC-SPS models derived from the Jind28 simulation (FC-only) compared with the Jindabyne data. FC-SPS 1 & 2 were set to represent endmember variants, each matching the data very well in certain respects, while FC-SPS 3 was chosen to represent the best balance between them. Not shown are FeO, CaO and K_2O vs. SiO_2, in which all models and the Jindabyne trends are approximately colinear.

match most trends including Fe_2O_3 vs. SiO_2 and achieve maximum SiO_2 of 67–68 wt% (compared to the 69 wt% in the Jindabyne Suite), but also leads to slight underestimation of Na_2O at a given SiO_2 content (Fig. 16). In contrast, using JndA65 and crystallinity thresholds of 9–12% yields stronger underestimation of Fe_2O_3 but less underestimation of Na_2O at a given SiO_2 content while only reaching SiO_2 contents as high as 65–66 wt%. It should also be noted that the over-enrichment of La and Nd (Fig. 13) is analogous to

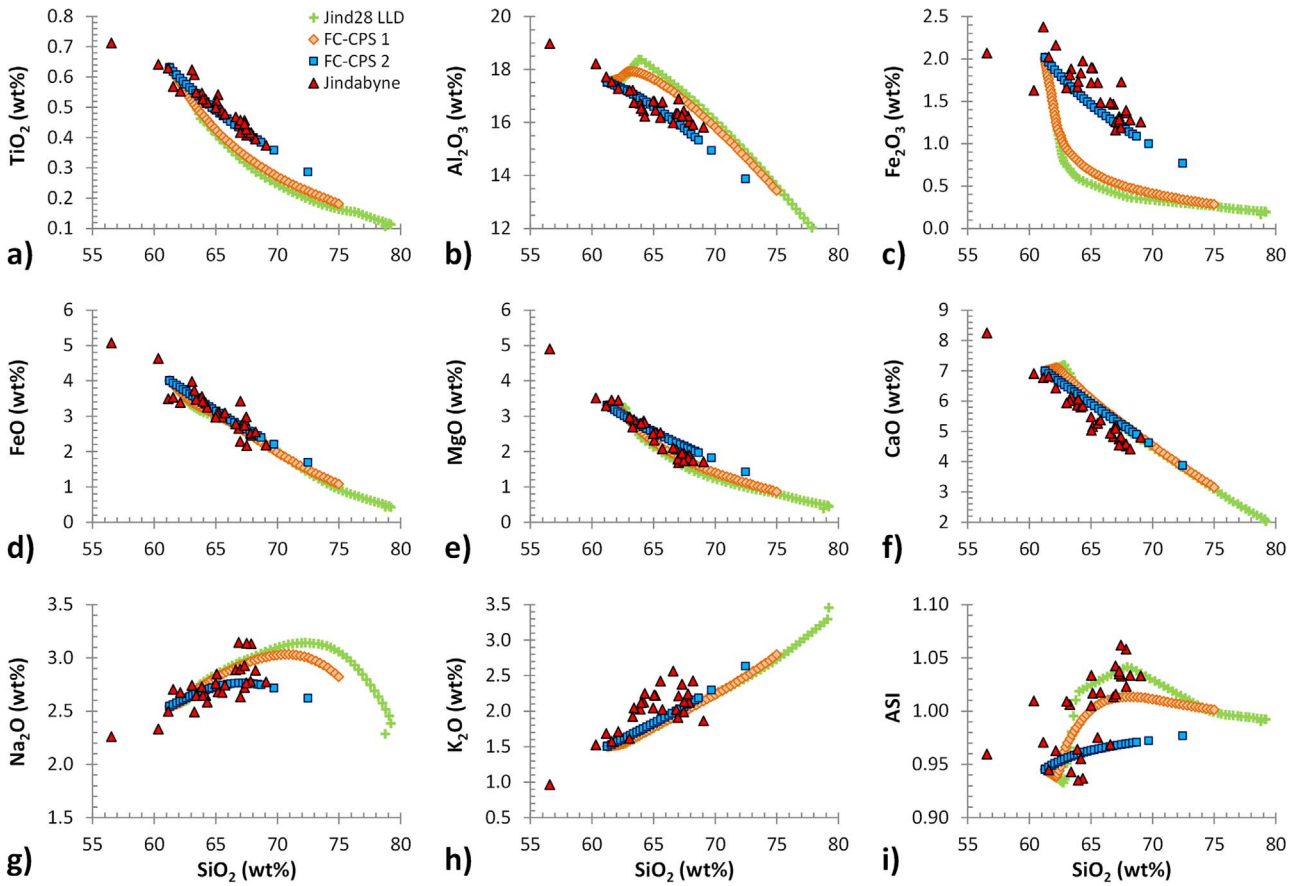

Fig. 15. FC-CPS models derived from the Jind28 simulation compared with the Jindabyne data. FC-CPS 1 & 2 represent endmember variants of concurrent partial segregation: in FC-CPS 1, 92% of the crystal cargo at each step is retained in the magma (8% is segregated from step to step of FC); in FC-CPS 2, no segregation occurs until the crystallinity reaches 32%, after which crystal segregation occurs at each step in maintain this crystallinity.

the strong depletion in Fe_2O_3, in the JndA65–67 LLDs, while most other trace elements LLD trends have a closer concordance with the Jindabyne data, and this concordance will carry over to the AFC-CPS trends as shown for major elements in Fig. 16.

In situ crystallisation

Conceptually, *in situ* crystallisation could be viewed as related to but one step removed from FC as a mechanism for magma evolution. Although MCS is not exactly designed to model this process, it can be used to build such models, and here we present an exploration of this possibility applied as one alternative model for the Jindabyne Suite.

Simulation Jind28 was chosen to provide the compositions of the fractionated liquids to be added to the resident magma. The evolution of the resident magma was calculated in steps involving: (1) separation of 20% of the resident magma mass to be crystallised to a specific degree (multiple crystallisation percentages were tested but kept constant across a single model), (2) division of the crystallisation zone into 10% 'trapped' liquid, the set percentage of crystals and the remainder being the fractionated liquid that gets mixed back into the resident magma, and (3) iterating with each new resident magma composition. The best fit to the Jindabyne Suite data was achieved by having 25% crystallisation in the crystallisation zone to produce the fractionated liquid, which means that in each step the new resident magma is 80:13 mix of old previous resident magma and fractionated liquid and the residue of the crystallisation zone is 25:10 crystals to fractionated liquid.

As shown in Fig. 17, the resident magma closely matches the data on most Harker diagrams and generally show very little curvature. The main issue with these trends is that a trade-off between the fit in TiO_2-Fe_2O_3-SiO_2 space and in Na_2O-ASI-SiO_2 space occurs in the *in situ* crystallisation models according to the degree of crystallisation (analogous to the trade-off controlled by degree of segregation in FC-CPS; Fig. 15).

DISCUSSION AND IMPLICATIONS

Assessment of models

The primary aim of the modelling discussed above was to see if FC could plausibly be the driver behind the major and trace element trends of the Jindabyne Suite. The remarkable consistency of linear variations in this and other suites has been considered by some to require a process such as restite unmixing that is designed to explain linear trends (White & Chappell, 1977; Hine *et al.*, 1978; Chappell *et al.*, 1987; Chappell, 1996). While FC does not a priori produce consistent linear geochemical variation, others have suggested that it could produce such trends for granitoid compositions and have integrated this into petrogenetic models (Wall *et al.*, 1987; Collins, 1996; Keay *et al.*, 1997; Jagoutz, 2010; Lee & Buchmann, 2014).

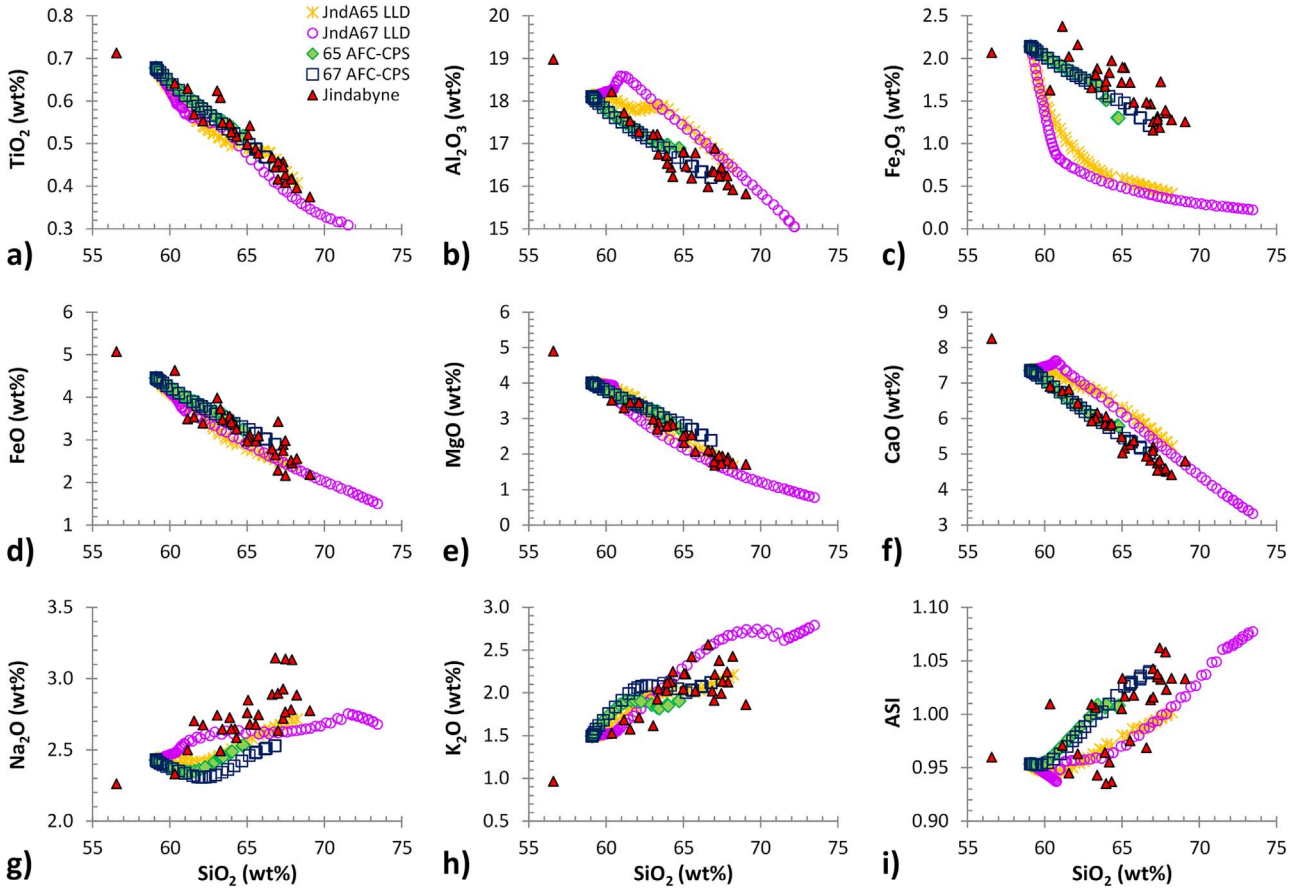

Fig. 16. AFC-CPS models derived from simulation JndA65 and JndA67 compared with the Jindabyne data. In both cases the segregation of crystals according to a crystallinity threshold resulted in the best fit to the data. Note that the main mismatches with the data occur for Na_2O and to a lesser extent for K_2O. Also, for the AFC-CPS model based on JndA65, starts to fall away from the Jindabyne Fe_2O_3-SiO_2 trend.

Across of a wide variety of magma starting compositions and conditions, FC simulated with the most sophisticated modelling tools available is unable to produce linear (or sensibly linear) relationships amongst all major element oxide concentrations for fractionated liquids of a broad compositional range (e.g. the 55–69 wt% SiO_2/1.7–4.8 wt% MgO range of the Jindabyne Suit; Figs 9 and 10). Consistent features of the LLDs of FC models are: curvature that cannot be accommodated by the scatter in the data; depletion of an oxide relative to the data across all or most of the SiO_2 range; and distinct kinks and inflection points that lead to gross deviations from the range and linearity of the data. The 'best fit' FC models, Jind18 and Jind22, overcome these issues only for certain bivariate element plots, but not others, and thus cannot be regarded as viable models for the Jindaybne Suite.

By exploring a wide range of different input parameters in AFC models it has been shown that geochemical trends broadly consistent with the Jindabyne Suite major element data can be produced as a series of liquids evolving by AFC; however, a few departures from the data are persistent despite extensive modelling focused on achieving the best possible fit (Fig. 12). Additionally, although deviations in modelled major element trends might be regarded as minor, more dramatic deviations arise for trace elements (Fig. 13). Thus, the modelling presented casts doubt upon the ability of AFC to produce liquid compositions consistent with the Jindabyne Suite.

While the LLDs for (A)FC are demonstrably inappropriate for reproducing the Jindabyne Suite geochemical trends, more promising results were shown for FC with subsequent or concurrent partial segregation and for FC-driven *in situ* crystallisation (Figs 14, 16 and 17). Geochemical trends for FC-SPS and *in situ* crystallisation based on simulation Jind28 and AFC-CPS based on JndA65–67 reproduce the Jindabyne Suite data reasonably well, albeit with some slight flaws. One key difference between them is the crystallinity of the magma and what crystals would be present given the cumulates required to produce the models.

In Jind28, magnetite is the first mineral to crystallise, then orthopyroxene, clinopyroxene, plagioclase, garnet and ilmenite appear on the liquidus after ~2, 3, 8, 26 and 47% crystallisation, respectively. Amphibole, quartz and biotite only appear in the last couple of steps of the simulation. The samples contain amphibole pseudomorphs after pyroxene (including relict clinopyroxene preserved in some amphibole), have magnetite as the main opaque phase, and have abundant plagioclase with calcic cores, but garnet is absent. By its nature FC-SPS produces magmas that all have a memory of the full range of cumulate phases – that is until overprinted by processes that might occur at emplacement level. The presence of garnet in simulation Jind28 is, therefore, a potential problem for the viability of FC-SPS as an explanation of Jindabyne. The preferred FC-SPS trend requires 34% crystallisation, at which

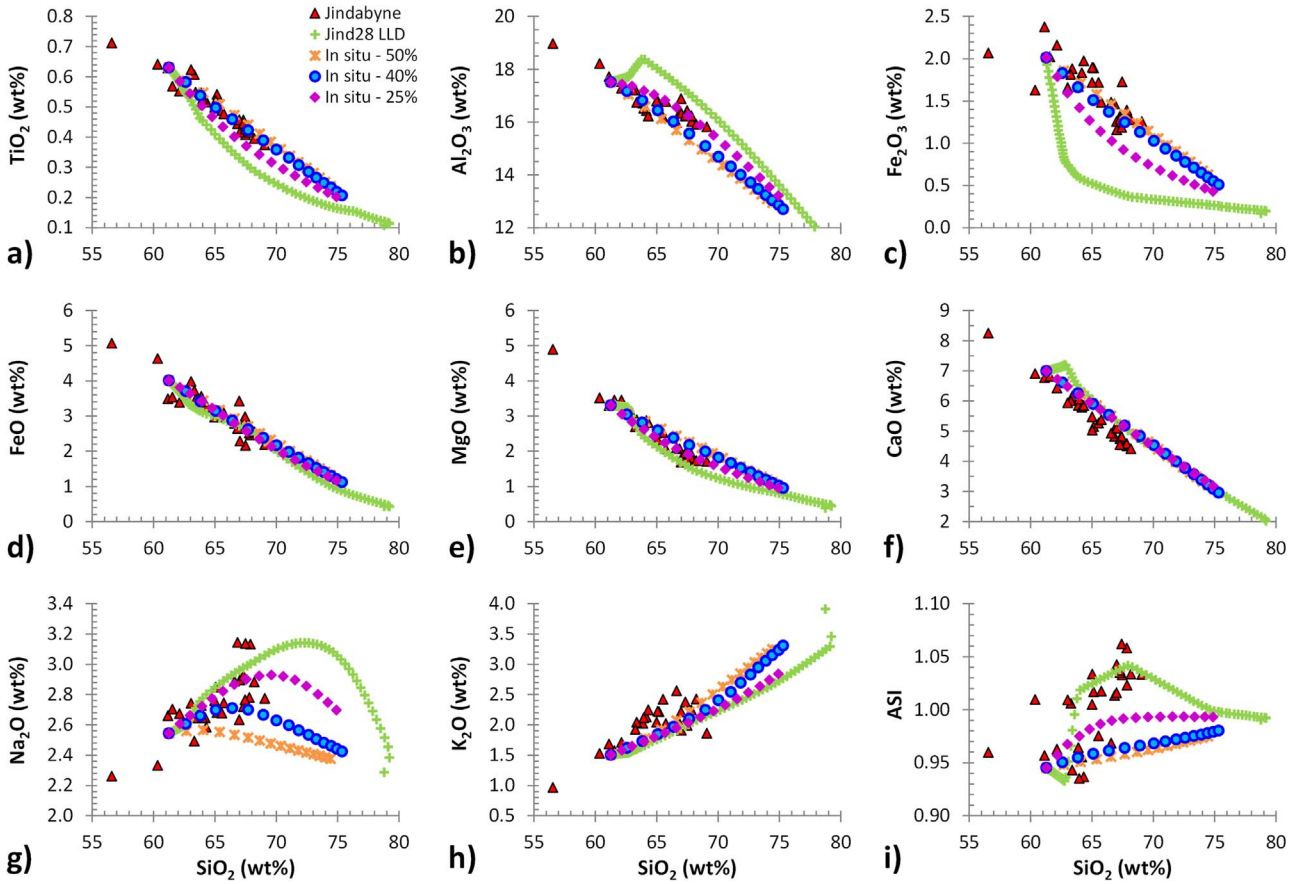

Fig. 17. *In situ* crystallisation models based on the Jind28 simulation (FC-only). The LLD shown corresponds to the starting magma and was used as a guide for the determining fractionated liquid compositions to be back-mixed into the resident magma. The percentages shown for each *in situ* model resident magma evolution indicate the degree of crystallisation that occurs in the crystallisation zone to produce the fractionated liquid in each step.

point garnet makes ~9% of the cumulate assemblage, compared to ~15 and 19% of the assemblage being ortho- and clinopyroxene, respectively. It is possible that reaction between the cumulate assemblage and the melt as the plutons cooled and solidified erased garnet and orthopyroxene while leaving vestiges of clinopyroxene (the more abundant of these), but this casts some doubt on the model. Alternatively, the presence of garnet in the model possibly reflects an issue in MELTS, associated with the known limitations in MELTS predicting the stability of amphibole (Ghiorso & Gualda, 2015). The experimental data of Naney (1983) and Dall'Agnol *et al.* (1999) suggest that amphibole might in fact crystallise within the 900–780°C, 8–10 wt% H_2O in the melt interval in which garnet crystallisation is predicted in this model. Even assuming amphibole instead of garnet ought to crystallise, since that temperature range is dominantly outside the range determined for the Jindabyne amphiboles, and the model is at a notably different pressure, this hypothetical amphibole would not be consistent with the amphibole compositions observed in the rocks. Thus, the requirement for a phase to be overwritten by reaction/re-equilibration would remain. *In situ* crystallisation, in contrast, produces a series of liquid resident magmas, crystallisation of which at the lower pressure of the emplacement level need not record the same mineral assemblage as the process that produced them; therefore, *in situ* crystallisation could be regarded as a more viable model for Jindabyne than FC-SPS. Indeed, simulations testing pressure variations showed that garnet would not be a cumulate phase at lower pressures, while pyroxenes and plagioclase still appear. Plagioclase with An content of 80 to 46 produced across the crystallisation range relevant to the FC-SPS models shown are consistent with the mineral compositions observed in the Jindabyne samples. Modelling suggests a drop in pressure from 350 to 250 MPa results in negligible change in the An content of the earliest-crystallised plagioclase; therefore, we posit that ascent of batches of the evolving resident magma of an *in situ* crystallisation model would produce phenocrystic plagioclase consistent with the observed core compositions. Nevertheless, if there is a problem with MELTS predicting the correct phase assemblage for Jind28, we cannot be sure that the correct magma evolution associated with the Jind28 conditions would fit the Jindabyne Suite data under either FC-SPS or *in situ* crystallisation.

Like FC-*SPS*, some memory of the cumulate phases would also be expected in magmas associated with AFC-*CPS*, although the crystal cargo would vary from sample to sample. Simulation JndA65 first crystallises magnetite, then orthopyroxene, plagioclase and finally clinopyroxene. The sequence is similar for JndA67, but clinopyroxene appears before plagioclase, and eventually ilmenite appears. Note that neither JndA65 nor JndA67 predict the involvement of garnet. Thus, the concerns discussed above for Jind28 do not arise. Simulations JndA65 and JndA67 crystallise plagioclase with anorthite contents of 80–73 and 83–55, respectively; therefore, either would be capable of explaining the calcic cores observed in the granite

samples. The main weaknesses of these in comparison to the FC-SPS and *in situ* crystallisation models are: (1) AFC-CPS models are more sensitive to the shape of the LLDs, causing curvature to trends on some plots that must be assumed to be hidden by scatter in data, and (2) they do not extend to high enough SiO_2 contents to explain the complete range of Jindabyne samples without introducing greater deviation from the data (in particular, both adding late-stage FC and extending the models by increasing WR mass lead to lowering of Na_2O at the felsic end). Nevertheless, in explicitly involving a cumulate assemblage in the magmas, the AFC-CPS models arguably are a more natural explanation than *in situ* crystallisation for the presence of distinct core domains in plagioclase and relict pyroxene in amphibole in the granites.

Ultimately, there are strengths and weakness to all of these alternatives, but the modelling demonstrates that they fit the Jindabyne data reasonably well (Figs 14, 16 and 17) and are broadly consistent with the observed mineral assemblages. Thus, the partial segregation and *in situ* crystallisation models are regarded as viable explanations for the major and trace element variations of the Jindabyne Suite, whereas derivation of the suite as an LLD of FC is not plausible.

Insights from models

Part of the long-running debate over the origin of granites in the LFB and NEFB, Australia, has been whether restite unmixing was responsible for the major and trace element variations within individual suites (be they individual plutons or groups of plutons) or whether FC in some form or other could be responsible. This sort of question is common to the investigation of the origins of any group of igneous rocks. This case study of the Jindabyne Suite serves as an example of how MCS can be used to address such questions.

The results of this study show that thermodynamically constrained FC does not produce linear or near linear LLDs for the compositional range of the Jindabyne Suite (Figs 9 and 10), contrary to the simplified model presented by Wall *et al.* (1987). This is true also when models are extended to include assimilation (Figs 12 and 13). Nevertheless, our modelling shows that near linear geochemical trends approximating the Jindabyne Suite data can be produced in models related to FC (partial segregation and *in situ* crystallisation models; Figs 14, 16 and 17); therefore, the modelling supports the assertion of Collins (1996) that FC offers a plausible alternative to restite unmixing as an explanation for LFB granite suites such as Jindabyne. It is yet to be seen, however, whether models such as (A)FC-SPS, (A)FC-CPS or *in situ* crystallisation would be fitting for any other specific suite of granitoids. Furthermore, for the 3-component mixing model of Collins (1996) to represent a comprehensive explanation of all the geochemical data, crystallisation-differentiation models such as these would need to be viable for more examples than just a few specific granitoid suites. It is not, however, clear if they *are* generally viable options to explain the linear geochemical variations so commonly seen in the LFB and NEFB.

One way to examine the broader question of the ability of (A)FC to produce the linear geochemical trends observed in LFB and NEFB I-types is to consider how easily this process produces a variety of curved and kinked LLDs. In order to produce major element trends as close as possible to the Jindabyne data, very specific combinations of magma composition and WR composition, initial temperature and mass were required. For many other combinations of parameters (including many of the exposed sedimentary rock compositions) the models deviate from the data on multiple plots. This suggests that, if AFC were a general process occurring again and again across as single region to produce granite suites representing LLDs, diverse, non-linear geochemical trends among granite suites should be common. This is in stark contrast to the observation that consistent linear variation is prevalent in the LFB granites.

Based on the example of the Jindabyne Suite modelling, FC (±assimilation) with imperfect liquid-crystal separation may be more suited than LLD models to producing linear and near-linear trends as the prevailing pattern in a granite province. The observation that (A)FC-CPS is somewhat sensitive to the shape of LLDs (Figs 1, 15 and 16) places some constraints on what form of partial segregation model would be best suited to the pattern of trends in the LFB. Having a threshold crystallinity before segregation of crystals occurs tends to produce simpler (A)FC-CPS trends than similar models with partial segregation throughout (unless segregation is very limited, which also limits the compositional range). Also, (A)FC-SPS models produce strictly linear trends for the same reason that restite unmixing does; therefore, it is in theory a more suitable candidate for a general, FC-driven mechanism for producing these sort of trends than (A)FC-CPS. The form of *in situ* crystallisation described, while not guaranteed to produce linear trends, does show less sensitivity to LLD shape than (A)FC-CPS. Finally, it should be noted that it cannot be taken for granted that some form FC (while viable for the Jindabyne Suite) is capable of accounting for the LFB and NEFB granite suites generally, as is done in petrogenetic models (see Introduction; Collins, 1996, Collins, 1998, Keay *et al.*, 1997, Kemp *et al.*, 2007).

Directions for future research

We suggest two broad lines of further research: continued investigation of Jindabyne Suite, and exploration of the general applicability of FC for producing linear geochemical trends.

The modelling conducted as part of this study narrows the large range of possibilities under the banner of 'fractional crystallisation' to a small set of detailed, potentially viable and testable explanations for the Jindabyne Suite. One way to test the presented FC-SPS, AFC-CPS and *in situ* crystallisation models and differentiate between them would be to conduct a study of trace element contents in minerals (particularly plagioclase cores and relict clinopyroxene) to compare with what would be expected for each of the models. Another would be to develop additional modelling tools that work with MCS to handle the behaviour of zircon and monazite and expand the sorts of trace element and isotopic data about which the models could be used to form testable hypotheses. To address the limitations of Rhyolite-MELTS with respect to stabilising water-rich phases, alternative modelling software could be employed to reassess the presented models.

Our case study could potentially be a blueprint for applying modern modelling tools to investigate geochemical trends in granite suites. Applying this approach to other granite suites in the LFB (such as Moruya, which has a similarly wide compositional range) could enhance our understanding of whether FC is generally applicable (and in what form) for producing a whole range of granite suites with linear trends. The example of this case study shows the potential to assess the likely trends that different FC-related processes would produce given the shape of a particular LLD. An exploratory study of geochemical evolutions of diverse granitic parental magmas could, therefore, also prove insightful.

It should also be recognised that, in contrast to the potential problems with invoking FC for these granites, the restite model readily explains linear geochemical trends. With this in mind, another avenue for research is to pursue investigations that could identify

other signatures of restite in these granites and to address whether the existing isotope data (McCulloch & Chappell, 1982; McCulloch & Woodhead, 1993; Keay *et al.*, 1997; Kemp *et al.*, 2006; Kemp *et al.*, 2007; Gray & Kemp, 2009; Iles *et al.*, 2020) can be reconciled with the restite model explanation for the major and trace element data.

CONCLUSIONS

Modelling conducted using the MCS demonstrates that the linear geochemical trends of the Jindabyne Suite cannot be explained as LLDs of FC with or without assimilation. The persistent deviations from linearity across the numerous simulated LLDs suggest that LLDs cannot be generally regarded as consistent with linear variation in granitoids. The modelling suggests the Jindabyne Suite trends can, however, be approximately reproduced by either (A)FC models involving different degrees of partial segregation of crystals from melt or FC-driven *in situ* crystallisation. Given the results of this study we suggest that the MCS may be useful for investigating the differentiation of other granitoids globally as well as for establishing the more generally applicability of FC as part of models for the LFB granite magmatism.

ACKNOWLEDGEMENTS

We would like to thank our colleagues, Aku Heinonen, Frank Spera, Riikka Fred and Ville Virtanen for many informative discussions about granites, modelling and thermodynamics. We would also like to thank Wendy Bohrson, whose advice as editor on an earlier version of this work helped to reshape and refocus it into a much improved manuscript. The final manuscript has benefited from the helpful guidance of the reviewers, Anastassia Borisova, Saskia Erdmann and Antonio Acosta-Vigil, and the editor, Marlina Elburg, who all have our gratitude.

FUNDING

This contribution has been funded by the Academy of Finland (Grant Nos. 295129 and 306962).

DATA AVAILABILITY STATEMENT

The data underlying this article are available in the article and in its online supplementary material.

SUPPLEMENTARY DATA

Supplementary data are available at *Journal of Petrology* online.

REFERENCES

Acosta-Vigil, A., Buick, I., Cesare, B., London, D. &Morgan, G. B., VI. (2012). The extent of equilibration between melt and residuum during regional anatexis and its implications for differentiation of the continental crust: a study of partially melted metapelitic enclaves. *Journal of Petrology* **53**, 1319–1356.

Adam, J. & Green, T. (2006). Trace element partitioning between mica- and amphibole-bearing garnet lherzolite and hydrous basanitic melt: 1. Experimental results and the investigation of controls on partitioning behaviour. *Contributions to Mineralogy and Petrology* **152**, 1–17.

Bacon, C. R. & Druitt, T. H. (1988). Compositional evolution of the zoned calcalkaline magma chamber of Mount Mazama, Crater Lake, Oregon. *Contributions to Mineralogy and Petrology* **98**, 224–256.

Bea, F., Pereira, M. D. & Stroh, A. (1994). Mineral/leucosome trace element partitioning in a peraluminous migmatite (a laser ablation-ICP-MS study). *Chemical Geology* **117**, 291–312.

Bédard, J. H. (2006). Trace element partitioning in plagioclase feldspar. *Geochimica et Cosmochimica Acta* **70**, 3717–3742.

Bédard, J. H. (2007). Trace element partitioning coefficients between silicate melts and orthopyroxene: parameterizations of D variations. *Chemical Geology* **244**, 266–303.

Behrens, H. & Gaillard, F. (2006). Geochemical aspects of melts: volatiles and redox behaviour. *Elements* **2**, 275–280.

Belousova, E. A., Griffin, W. L. & O'Reilly, S. Y. (2006). Zircon crystal morphology, trace element signatures and Hf isotope composition as a tool for petrogenetic modelling: examples from eastern Australian granitoids. *Journal of Petrology* **47**, 329–353.

Bohrson, W. A., Spera, F. J., Ghiorso, M. S., Brown, G. A., Creamer, J. B. & Mayfield, A. (2014). Thermodynamic model for energy-constrained open-system evolution of crustal magma bodies undergoing simultaneous recharge, assimilation and crystallization: the Magma Chamber Simulator. *Journal of Petrology* **55**, 1685–1717.

Brophy, J. G., Ota, T., Kunihiro, T., Tsujimori, T. & Nakamura, E. (2011). In situ ion-microprobe determination of trace element partition coefficients for hornblende, plagioclase, orthopyroxene, and apatite in equilibrium with natural rhyolitic glass, Little Glass Mountain Rhyolite, California. *American Mineralogist* **96**, 1838–1850.

Bowes. (1954). The metamorphic and igneous history of Rosetta Head, South Australia. *Transactions of the Royal Society of South Australia* **77**, 182–214.

Chappell, B. W. (1984). Source rocks of I- and S-type granites in the Lachlan Fold Belt, southeastern Australia. *Philosophical Transactions of the Royal Society of London* **A310**, 693–706.

Chappell, B. W. (1996). Compositional variation within granite suites of the Lachlan Fold Belt: its causes and implications for the physical state of granite magma. *Transactions of the Royal Society of Edinburgh: Earth Sciences* **87**, 159–170.

Chappell, B. W. & Stephens, W. E. (1988). Origin of infracrustal (I-type) granite magmas. *Transactions of the Royal Society of Edinburgh: Earth Sciences* **79**, 71–86.

Chappell, B. W. & White, A. J. R. (1992). I- and S-type granites in the Lachlan Fold Belt. *Transactions of the Royal Society of Edinburgh: Earth Sciences* **83**, 1–26.

Chappell, B. W. & White, A. J. R. (2001). Two contrasting granite types: 25 years later. *Australian Journal of Earth Sciences* **48**, 489–499.

Chappell, B. W., White, A. J. R. & Wyborn, D. (1987). The importance of residual source material (restite) in granite petrogenesis. *Journal of Petrology* **28**, 1111–1138.

Chen, Y. D. & Williams, I. S. (1990). Zircon inheritance in mafic inclusions from Bega batholith granites, southeastern Australia: an ion microprobe study. *Journal of Geophysical Research* **95**, 17787–17796.

Chen, Y. D., Price, R. C. & White, A. J. R. (1989). Inclusions in three S-type granites from southeastern Australia. *Journal of Petrology* **30**, 1181–1218.

Chen, Y. D., Chappell, B. W. & White, A. J. R. (1991) Mafic enclaves of some I-type granites of the Palaeozoic Lachlan Fold Belt, south-eastern Australia. In: (Didier J. & Barbarin B. (eds)) *Enclaves and Granite Petrology*. Amsterdam: Elsevier Science Publishers B.V, pp.113–124.

Clemens, J. D. & Stevens, G. (2012). What controls chemical variation in granitic magmas? *Lithos* **134–135**, 317–329.

Collins, W. J. (1996). Lachlan Fold Belt granitoids: products of three-component mixing. *Transactions of the Royal Society of Edinburgh: Earth Sciences* **87**, 171–181.

Collins, W. J. (1998). Evaluation of petrogenetic models for Lachlan Fold Belt granitoids: implications for crustal architecture and tectonic models. *Australian Journal of Earth Sciences* **45**, 483–500.

Collins, W. J., Murphy, J. B., Johnson, T. E. & Huang, H.-Q. (2020). Critical role of water in the formation of the continental crust. *Nature Geoscience* **13**, 331–338.

Compston, W. & Chappell, B. W. (1979) Sr-isotope evolution of granitoid source rocks. In: (McElhinny M. W. (ed)) *The Earth: Its Origin, Structure and Evolution*. London: Academic Press.

Dall'Agnol, R., Scaillet, B. & Pichavant, M. (1999). An experimental study of a lower Proterozoic A-type granite from the eastern Amazonian craton, Brazil. *Journal of Petrology* **40**, 1673–1698.

Dalpé, C. & Baker, D. R. (2000) Experimental investrigation of large-ion-lithophile-element-, high-field-strength-element-, and rare-earth-element-partitioning between calcic amphibole and basaltic melt; the effects of pressure and oxygen fugacity. *Contributions to Mineralogy & Petrology*. **140**, 233–350.

DePaolo, D. J. (1981). Trace element and isotopic effects of combined wallrock assimilation and fractional crystallization. *Earth and Planetary Science Letters* **53**, 189–202.

Dorais, M. J. & Spencer, C. J. (2014). Revisiting the importance of residual source material (restite) in granite petrogenesis: the Cardigan Pluton, New Hampshire. *Lithos* **202–203**, 237–249.

Dwarzski, R., Draper, D., Shearer, C. & Agee, C. (2006). Experimental insights on crystal chemistry of high-Ti garnets from garnet-melt partitioning of rare-earth and high-field-strength elements. *American Mineralogist* **91**, 1536–1546.

Ewart, A. & Griffin, W. L. (1994). Application of proton-microprobe data to trace-element partitioning in volcanic rocks. *Chemical Geology* **117**, 251–284.

Fabbrizio, A., Schmidt, M. W., Günther, D. & Eikenberg, J. (2008). Experimental determination of radium partitioning between leucite and phonolite melt and 226Ra-disequilibrium crystallization ages of leucite. *Chemical Geology* **255**, 377–397.

Farina, F. & Stevens, G. (2011). Source controlled $^{87}Sr/^{86}Sr$ isotope variability in granitic magmas: the inevitable consequence of mineral-scale isotopic disequilibrium in the protolith. *Lithos* **122**, 189–200.

Fergusson, C. L. & Coney, P. J. (1992). Implications of a Bengal fan-type deposit in the Paleozoic Lachlan fold belt of southeastern Australia. *Geology* **20**, 1047–1049.

Ghiorso, M. S. (1985). Chemical mass transfer in magmatic processes I. thermodynamic relations and numerical algorithms. *Contributions to Mineralogy and Petrology* **90**, 107–120.

Ghiorso, M. S. & Gualda, G. A. R. (2015) Chemical thermodynamics and the study of magmas. In: (Sigurdsson H. (ed)) *The Encyclopedia of Volcanoes*, Second edn. Amsterdam: Elsevier, pp.143–161.

Ghiorso, M. S. & Sack, R. O. (1995). Chemical mass transfer in magmatic processes IV. A revised and internally consistent thermodynamic model for the interpolation and extrapolation of liquid-solid equilibria in magmatic systems at elevated temperatures and pressures. *Contributions to Mineralogy and Petrology* **119**, 197–212.

Gray, C. M. (1984). An isotopic mixing model for the origin of granitic rocks in southeastern Australia. *Earth and Planetary Science Letters* **70**, 47–60.

Gray, D. R. & Foster, D. A. (2004). Tectonic evolution of the Lachlan Orogen, Southeast Australia: historical review, data synthesis and modern perspectives. *Australian Journal of Earth Sciences* **51**, 773–817.

Gray, C. M. & Kemp, A. I. S. (2009). The two-component model for the genesis of granitic rocks in southeastern Australia – nature of the metasedimentary-derived and basaltic end members. *Lithos* **111**, 113–124.

Gualda, G. A. R., Ghiorso, M. S., Lemons, R. V. & Carley, T. L. (2012). Rhyolite-MELTS: a modified calibration of MELTS optimized for silica-rich, fluid-bearing magmatic systems. *Journal of Petrology* **53**, 875–890.

Healy, B., Collins, W. J. & Richards, S. W. (2004). A hybrid origin for Lachlan S-type granites: the Murrumbidgee Batholith example. *Lithos* **78**, 197–216.

Heinonen, J. S., Bohrson, W. A., Spera, F. J., Brown, G. A., Scruggs, M. A. & Adams, J. V. (2020). Diagnosing open-system magmatic processes using the Magma Chamber Simulator (MCS): part II—trace elements and isotopes. *Beiträge zur Mineralogie und Petrographie* **175**.

Hertogen, J. & Mareels, J. (2016). SilMush: a procedure for modeling of the geochemical evolution of silicic magmas and granitic rocks. *Geochimica et Cosmochimica Acta* **185**, 498–527.

Hill, E., Blundy, J. & Wood, B. (2011). Clinopyroxene-melt trace element partitioning and the development of a predictive model for HFSE and Sc. *Contributions to Mineralogy & Petrology* **161**, 423–438.

Hine, R., Williams, I. S., Chappell, B. W. & White, A. J. R. (1978). Contrasts between I- and S-type granitoids of the Kosciusko Batholith. *Australian Journal of Earth Sciences* **25**, 219–234.

Hogan, J. P. & Sinha, A. K. (1991). The effect of accessory minerals on the redistribution of lead isotopes during crustal anatexis: a model. *Geochimica et Cosmochimica Acta* **55**, 335–348.

Ickert, R. B. & Williams, I. S. (2011). U-Pb zircon geochronology of Silurian-Devonian granites in southeastern Australia: implications for the timing of the Benambran orogeny and the I-S dichotomy. *Australian Journal of Earth Sciences* **58**, 501–516.

Iles, K. A. (2017) *Isotopic Disequilibrium in Granitic Systems: The Origins of Heterogeneity in Granites and Implications for Partial Melting in the Crust and Petrogenetic Models*. In: *Melbourne: School of Earth Sciences*. The University of Melbourne.

Iles, K. A., Hergt, J. M. & Woodhead, J. D. (2018). Modelling isotopic responses to disequilibrium melting in granitic systems. *Journal of Petrology* **59**, 87–113.

Iles, K. A., Hergt, J. M., Woodhead, J. D., Ickert, R. B. & Williams, I. S. (2020). Petrogenesis of granitoids from the Lachlan Fold Belt, southeastern Australia: the role of disequilibrium melting. *Gondwana Research* **79**, 87–109.

Jacobsen, S. B. & Wasserburg, G. J. (1980). Sm-Nd isotopic evolution of chondrites. *Earth and Planetary Science Letters* **50**, 139–155.

Jagoutz, O. E. (2010). Construction of the granitoid crust of an island arc. Part II: a quantitative petrogenetic model. *Contributions to Mineralogy and Petrology* **160**, 359–381.

Keay, S. M., Collins, W. J. & McCulloch, M. T. (1997). A three-component Sr-Nd isotopic mixing model for granitoid genesis, Lachlan Fold Belt, eastern Australia. *Geology* **25**, 307–310.

Kemp, A. I. S., Whitehouse, M. J., Hawkesworth, C. J. & Alarcon, M. K. (2005). A zircon U-Pb study of metaluminous (I-type) granites of the Lachlan Fold Belt, southeastern Australia: implications for the high/low temperature classification and magma differentiation processes. *Contributions to Mineralogy and Petrology* **150**, 230–249.

Kemp, A. I. S., Hawkesworth, C. J., Paterson, B. A., Foster, G. L., Kinny, P. D., Whitehouse, M. J., Maas, R. & EIMF. (2006). Exploring the plutonic-volcanic link: a zircon U-Pb, Lu-Hf and O isotope study of paired volcanic and granitic units from southeastern Australia. *Transactions of the Royal Society of Edinburgh: Earth Sciences* **97**, 337–355.

Kemp, A. I. S., Hawkesworth, C. J., Foster, J. L., Paterson, B. A., Woodhead, J. D., Hergt, J. M., Gray, C. M. & Whitehouse, M. J. (2007). Magmatic and crustal differentiation history of granitic rocks from Hf-O isotopes in zircon. *Science* **315**, 980–983.

Kleine, M., Stosch, G.-H., Seck, H. A. & Shimizu, N. (2000). Experimental partitioning of high field strength and rare earth elements between clinopyroxene and garnet in andesitic to tonalitic systems. *Geochimica et Cosmochimica Acta* **64**, 99–115.

Klemme, S., Blundy, J. & Wood, B. (2002). Experimental constraints on major and trace element partitioning during partial melting of eclogite. *Geochimica et Cosmochimica Acta* **66**, 3109–3123.

Klemme, S., Günther, D., Hametner, K., Prowatke, S. & Zack, T. (2006). The partitioning of trace elements between ilmenite, ulvospinel, armalcolite and silicate meltis with implications for the early differentiation of the moon. *Chemical Geology* **234**, 251–263.

Koepke, J., Falkenberg, G., Rickers, K. & Diedrich, O. (2003). Trace element diffusion and element partitioning between garnet and andesite melt using synchrotron X-ray fluorescence microanalysis (μ-SRXRF). *European Journal of Mineralogy* **15**, 883–892.

Krawczynski, M. J., Grove, T. L. & Behrens, H. (2012). Amphibole stability in primitive arc magmas: effects of temperature, H2O content, and oxygen fugacity. *Une chaire de médecine au XVe siècle; un professeur à l'Université de Pavie de 1432 à 1472* **164**, 317–339.

Le Maitre, R. W. (ed) (2002) *Igneous Rocks: A Classification and Glossary of Terms*. Cambridge: Cambridge University Press.

Lee, C. -T. A. & Buchmann, O. (2014). How important is the role of crystal fractionation in making intermediate magmas? Insights from Zr and P systematics. *Earth and Planetary Science Letters* **393**, 266–274.

London, D., Morgan, G. B. & Acosta-Vigil, A. (2012). Experimental simulations of anatexis and assimilation involving metapelite and granitic melt. *Lithos* **153**, 292–307.

Luhr, J. F. & Carmichael, I. S. E. (1980). The Colima volcanic complex, Mexico: I. post-caldera andesites from Volcán Colima. *Contributions to Mineralogy and Petrology* **71**, 343–372.

Maas, R., Nicholls, I. A. & Legg, C. (1997). Igneus and metamorphic enclaves in the S-type Deddick Granodiorite, Lachlan Fold Belt, SE Australia: petrographic, geochemical and Nd-Sr isotopic evidence for crustal melting and magma mixing. *Journal of Petrology* **38**, 815–841.

Marks, M., Halama, R., Wenzel, T. & Markl, G. (2004). Trace element vairations in clinopyroxene and amphibole from alkaline to peralkaline syenites and granites; implications for mineral-melt trace-element partitioning. *Chemical Geology* **211**, 185–215.

McCarthy, T. S. & Robb, L. J. (1978). On the relationship between cumulus mineralogy and trace and alkali element chemistry in an Archean granite from the Barberton region, South Africa. *Geochimica et Cosmochimica Acta* **42**, 21–26.

McCulloch, M. T. & Chappell, B. W. (1982). Nd isotopic characteristics of S- and I-type granites. *Earth and Planetary Science Letters* **58**, 51–64.

McCulloch, M. T. & Woodhead, J. D. (1993). Lead isotopic evidence for deep crustal-scale fluid transport during granite petrogenesis. *Geochimica et Cosmochimica Acta* **57**, 659–674.

McKenzie, D. & O'Nions, R. K. (1991). Partial melt distributions from inversion of rare earth element concentrations. *Journal of Petrology* **32**, 1021–1091.

Milnes, A. R. (1973). *The Encounter Bay Granites, South Australia, and Their Environment*. *Adelaide: Department of Geology and Mineralogy*, The University of Adelaide.

Minissale, S., Zanetti, A., Tedesco, D., Morra, V. & Melluso, L. (2019). The petrology and geochemistry of Nyiragongo lavas of 2002, 2016, 1977 and 2017 AD, and the trace element partitioning between melilitite glass and melilite, nepheline, leucite, clinopyroxene, apatite, olivine and Fe-Ti oxides: a unique scenario. *Lithos* **332-333**, 296–311.

Naney, M. T. (1983). Phase equilibria of rock-forming ferromagnesian silicates in granitic systems. *American Journal of Science* **283**, 993–1033.

Nash, W. P. & Crecraft, H. R. (1985). Partition coefficients for trace elements in silicic magmas. *Geochimica et Cosmochimica Acta* **49**, 2309–2322.

Nathan, S. (1976). Geochemistry of the Greenland group (early Ordovician), New Zealand. *New Zealand Journal of Geology and Geophysics* **19**, 683–706.

Nehring, F., Foley, S. F. & Hölttä, P. (2010). Trace element partitioning in the granulite facies. *Contributions to Mineralogy and Petrology* **159**, 493–519.

Nielson, R. L., Gallahan, W. E. & Newberger, F. (1992). Experimentally determined mineral-melt partition coefficients for Sc, Y and REE for olivine, orthopyroxene, pigeonite, magnetite and ilmenite. *Contributions to Mineralogy and Petrology* **110**, 488–499.

Nishimura, K. & Yanagi, T. (2000). In situ crystallization observed in the Osumi granodiorite batholith. *Earth and Planetary Science Letters* **180**, 185–199.

O'Neil, J. R. & Chappell, B. W. (1977). Oxygen and hydrogen isotope relations in the Berridale Batholith. *Journal of the Geological Society of London* **133**, 559–571.

Owen, M. & Wyborn, D. (1979) *Geology and Geochemistry of the Tantangara and Bridabella 1:100000 Sheet Areas*. Canberra: Australian Government Publishing Service.

Philpotts, J. A. & Schnetzler, C. C. (1970). Phenocryst-matrix partition coefficients for K, Rb, Sr and Ba, with applications to anorthosite and basalt genesis. *Geochimica et Cosmochimica Acta* **34**, 307–322.

Pupier, E., Barbey, P., Toplis, M. J. & Bussy, F. (2008). Igneous layering, fractional crystallization and growth of granitic plutons: the Dolbel batholith in SW Niger. *Journal of Petrology* **49**, 1043–1068.

Rapp, R. P., Ryerson, F. J. & Miller, C. F. (1987). Experimental evidence bearing on the stability of monazite during crustal anatexis. *Geophysical Research Letters* **14**, 307–310.

Ren, M., Parker, D. F. & White, J. C. (2003). Partitioning od Sr, Ba, Rb, Y, and LREE between plagioclase and peraluminous silicic magma. *American Mineralogist* **88**, 1091–1103.

Ridolfi, F. (2021). Amp-TB2: an updated model for calcic amphibole Thermobarometry. *Minerals* **11**, 324.

Rubatto, D. & Hermann, J. (2007). Experimental zircon/melt and zircon/garnet trace element partitioning and implications for the geochronology of crustal rocks. *Chemical Geology* **241**, 38–61.

Sha, L.-K. & Chappell, B. W. (1999). Apatite chemical composition, determined by electron microprobe and laser-ablation inductively coupled plasma mass spectrometry, as a probe into granite petrogenesis. *Geochimica et Cosmochimica Acta* **63**, 3861–3881.

Shimizu, H. (1980). Experimental study on rare-earth element partitioning in minerals formed at 20 and 30 kb for basaltic systems. *Geochemical Journal* **14**, 185–202.

Sisson, T. W. & Grove, T. L. (1993). Experimental investigations of the role of H2O in calc-alkaline differentiation and subduction zone magmatism. *Contr Mineral and Petrol* **113**, 143–166.

Soesoo, A. (2000). Fractional crystallization of mantle-derived melts as a mechanism for some I-type granite petrogenesis: an example from Lachlan Fold Belt, Australia. *Journal of the Geological Society, London* **157**, 135–149.

Sweeney, R. J., Green, D. H. & Sie, S. H. (1992). Trace and minor element partitioning between garnet and amphibole and carbonatitic melt. *Earth and Planetary Science Letters* **113**, 1–14.

Tang, M., Wang, X.-L., Shu, X.-J., Wang, D., Yang, T. & Gopon, P. (2014). Hafnium isotopic heterogeneity in zircons from granitic rocks: geochemical evaluation and modelling of "zircon effect" in crustal anatexis. *Earth and Planetary Science Letters* **389**, 188–199.

Tuff, J. & Gibson, S. (2007). Trace-element partitioning between garnet, clinopyroxene and Fe-rich picritic melts at 3 to 7 GPa. *Contributions to Mineralogy and Petrology* **153**, 369–387.

Turner, S., Foden, J., Sandiford, M. & Bruce, D. (1993). Sm-Nd isotopic evidence for the provenance of sediments from the Adelaide Fold Belt and southeastern Australia with implications for episodic crustal addition. *Geochimica et Cosmochimica Acta* **57**, 1837–1856.

van Kan Parker, M., Mason, P. R. D. & van Westrenen, W. (2011). Trace element partitioning between ilmenite, armalcolite and anhydrous silicate melt: implications for the formation of lunar high-Ti mare basalts. *Geochimica et Cosmochimica Acta* **75**, 4179–4193.

Wall, V. J., Clemens, J. D. & Clarke, D. B. (1987). Models for granitoid evolution and source compositions. *The Journal of Geology* **95**, 731–749.

Whalen, J. B. & Chappell, B. W. (1988). Opaque mineralogy and mafic mineral chemistry of the I- and S-type granites of the Lachlan Fold Belt, southeastern Australia. *American Mineralogist* **73**, 281–296.

White, A. J. R. (2002). Bowen's reaction principle and the evolution of granite mineralogy. *The Australian Geologist* **125**, 7–10.

White, A. J. R. & Chappell, B. W. (1977). Ultrametamorphism and granitoid genesis. *Tectonophysics* **43**, 7–22.

White, A. J. R. & Chappell, B. W. (1988). Some supracrustal (S-type) granites of the Lachlan Fold Belt. *Transactions of the Royal Society of Edinburgh: Earth Sciences* **79**, 169–181.

White, A. J. R. & Chappell, B. W. (1989) *Geology of the Numbla 1:100000 Sheet 8624*. Sydney: New South Wales Geological Survey.

White, A. J. R., Williams, I. S. & Chappell, B. W. (1976). The Jindabyne thrust and its tectonic, physiographic and petrogenetic significance. *Journal of the Geological Society of Australia* **23**, 105–112.

White, A. J. R., Williams, I. S. & Chappell, B. W. (1977) *Geology of the Berridale 1:100000 Sheet*. Sydney: Geological Survey of New South Wales.

Williams, I. S. (1992). Some observations on the use of zircon U-Pb geochronology in the study of granitic rocks. *Transactions of the Royal Society of Edinburgh: Earth Sciences* **83**, 447–458.

Williams, I. S., Compston, W. & Chappell, B. W. (1983). Zircon and monazite U-Pb systems and the histories of I-type magmas, Berridale Batholith, Australia. *Journal of Petrology* **24**, 76–97.

Wood, B. J. & Trigila, R. (2001). Experimental determination of aluminous clinopyroxene-melt partition coefficients for potassic liquids, with application to the evolution of the Roman province potassic magmas. *Chemical Geology* **172**, 213–223.

Wyborn, D. (1992). The tectonic significance of Ordovician magmatism in the eastern Lachlan Fold Belt. *Tectonophysics* **214**, 177–192.

Wyborn, L. A. I. & Chappell, B. W. (1983). Chemistry of the Ordovician and Silurian greywackes of the Snowy Mountains, southeastern Australia: an example of chemical evolution of sediments with time. *Chemical Geology* **39**, 81–92.

Wyborn, D., Chappell, B. W. & James, M. (2001). Examples of convective fractionation in high-temperature granites from the Lachlan Fold Belt. *Australian Journal of Earth Sciences* **48**, 531–541.

Zeng, L., Asimow, P. D. & Saleeby, J. B. (2005). Coupling of anatectic reactions and dissolution of accessory phases and the Sr and Nd isotope systematics of anatectic melts from a metasedimentary source. *Geochimica et Cosmochimica Acta* **69**, 3671–3682.

Zhao, K., Xu, X. & Erdmann, S. (2018). Thermodynamic modeling for an incrementally fractionated granite magma system: implications for the origin of igneous charnockite. *Earth and Planetary Science Letters* **499**, 230–242.